Introduction: Mediterranean Climate—Background Information

Piero Lionello[a,b], Fatima Abrantes[c], Letizia Congedi[a], Francois Dulac[d], Miro Gacic[e], Damià Gomis[f], Clare Goodess[g], Holger Hoff[h], Haim Kutiel[i], Jürg Luterbacher[j], Serge Planton[k], Marco Reale[a], Katrin Schröder[l], Maria Vittoria Struglia[m], Andrea Toreti[n,o], Michael Tsimplis[p], Uwe Ulbrich[q], Elena Xoplaki[n,o]

[a]DISTEBA Department of Science and technology for Biology and The Environment, University of Salento, Lecce, Italy, [b]CMCC, Centro EuroMediterraneao per i Cambiamenti Climatici, Lecce, Italy, [c]Laboratório Nacional de Energia e Geologia, Unidade de Geologia Marinha, Amadora, Portugal, [d]IPSL, LSCE (CEA-CNRS-UVSQ) Gif-Sur-Yvette, and LISA (UPEC-UPDP7-CNRS), Créteil, France, [e]OGS, Trieste, Italy, [f]IMEDEA (Universitat de les Illes Balears, CSIC), Mallorca, Spain, [g]Climatic Research Unit, University of East Anglia, UK, [h]Potsdam Institute for Climate Impact Research, Germany and Stockholm Environment Institute, Sweden, [i]Department of Geography and Environmental Studies, University of Haifa, Haifa, Israel, [j]Department of Geography, Justus Liebig University, Climatology, Climate, Giessen, Germany, [k]CNRM-GAME, Météo France, Toulouse, France, [l]CNR-ISMAR, La Spezia, Italy, [m]ENEA, Rome, Italy, [n]Department of Geography, Climatology, Climate Dynamics and Climate Change, Justus-Liebig University of Giessen, Giessen, Germany, [o]Institute of Geography, Climatology and Meteorology, University of Bern, Bern, Switzerland, [p]National Oceanography Centre Southhampton, Southampton, UK, [q]Freie Universität, Berlin, Germany

I.1 Introduction

This introductory chapter presents general and consolidated background knowledge to be referred to in the rest of the book and anticipates, though only partially, the information that is provided in the book chapters, where a complete description of scientific issues and recent research results is presented, including technical details and discussion of open issues. The content intends not only to reflect what is known about Mediterranean climate but also to highlight the open issues associated with limitations in data availability or lack of understanding of key processes. It provides essential information, which is not limited to basic climate variables, such as surface temperature and precipitation, but reflects the complexity of the climate system, the role of the main subsystems and factors, and includes also the links among environment, society, and climate.

The Mediterranean Sea is the crucial environmental factor in this region. The presence of a large marginal and almost completely closed sea on the western side of a large continental area is geographically unique. Its size is actually substantial. Its area, excluding the Black Sea, is about 2.5 million km^2. Its extent is about 3700 km in longitude and 1600 km in latitude and has an average depth of 1500 m. The Strait of Gibraltar, connecting the Mediterranean Sea to the Atlantic is only 14.5 km wide and less than 300 m deep at the shallowest sill. These morphological characteristics make the Mediterranean Sea a large source of moisture and a heat reservoir with a significant capacity for the surrounding land areas (considering the annual average, it acts as a moderate source of heat). The Strait of Gibraltar plays a crucial role for the environment of the Mediterranean Sea. The fluxes through the strait compensate for the mass deficit due to the large evaporation in the basin, supply comparatively freshwater masses to one of the saltiest seas on Earth, and also provide a small supply of heat, because the Mediterranean water (MW) outflow is cooler than the Atlantic water (AW) inflow. The complicated morphology of the region—with its many sharp orographic features, often close to the coastlines, and the presence of distinct basins and gulfs, islands, and peninsulas—has a strong effect on the atmospheric circulation. It is responsible for several cyclogenetic areas, local winds, many mesoscale processes, and intense air–sea interactions, such as those responsible for dense-water formation processes driving the Mediterranean thermohaline cells. Further, the shape of the Mediterranean Sea bottom, with deep basins linked through much shallower straits, strongly constrains the Mediterranean Sea circulation.

The sequence of the sections in this introductory chapter is meant to follow the logic of the Mediterranean Climate Variability and Predictability (MedCLIVAR) project, merging the different topics and timescales that are needed for a comprehensive description of the Mediterranean climate. This is a region with large socioeconomic contrasts and sectors that are very vulnerable to climate change (Section I.2). Though this book and MedCLIVAR do not actually deal with socioeconomic issues, it is important to be aware of the information that is needed by policymakers and stakeholders in the Mediterranean region. Some general characteristics of the Mediterranean region are described in Section I.3. Specifically, it is well known that reaching the spatial resolution required to study local impacts is a formidable task for which climate research is required to dedicate a strong effort, especially for the Mediterranean region, where environmental and morphological gradients are particularly large. Sections I.4–I.8 describe past evolution of the climate and its present condition and trends. Its complicated past evolution (Section I.4), with dramatic events that have left clear marks in the Mediterranean geological history, is by itself a fascinating research subject with interesting specific problems (Section I.4), but also poses the problem of whether any of these past conditions, such as the anoxic states documented in the past, can occur again in the next decades and centuries. The presence of archeological records since ancient times and documentary proxies to complement the natural archives offers a unique (with the only possible exception of China) opportunity for reconstructing the climate in historical times (Section I.5). The interpretation of this information is not straightforward, but gives to the Mediterranean region an exceptional opportunity to assess whether the recent pace of climate variations is unprecedented in the history of the past millennia. Trends in temperature and precipitation (Sections I.6 and I.8) have been observed in the twentieth century and for temperature their consistency with global warming is not controversial, even if a demonstration of the consistency between the patterns in observations and climate simulations remains challenging (Section I.17).

Sections I.9–I.15 describe components and factors and their Mediterranean specificities, beginning with the marine component. The Mediterranean Sea circulation (Section I.9) presents three main thermohaline cells driven by dense-water formation: a basinwide open cell, with a freshwater inflow from the Atlantic counteracted by a salty outflow of water formed in the Levantine basin across the Gibraltar Strait, and two separated closed cells, one for the western and one for the eastern part of the basin. This last one is peculiar, as it has been observed that it can operate in two different regimes, with dense-water formation in different areas, which are suggestive of possible multiple equilibriums. The shift of the formation site of deep waters from the Adriatic to the Aegean took place in the late 1980s and it is called EMT (eastern Mediterranean transient). The Mediterranean Sea level (Section I.10) has been shown to depart in its trends and variability from the nearby Atlantic Ocean, because of important local factors, which make it very uncertain to link its evolution to that of global sea level for the next decades.

Rivers, atmospheric cyclones, winds, ocean waves, and aerosols are briefly discussed in Sections I.11–I.15. Rivers (Section I.11) are a key component to close the hydrological cycle and the mass balance of the Mediterranean Sea. Atmospheric cyclones in the Mediterranean (Section I.12) determine a separate branch of the northern hemisphere storm track, with several areas of cyclogenesis, mainly in the western Mediterranean, and prevalent cyclolysis in the central and eastern Mediterranean. Spatially and seasonally varying wind regimes are summarized in Section I.13. Ocean waves (Section I.14) are a factor to be accounted for the management and evolution of the coasts. A high aerosol load over the basin, dominated by continental sources, significantly impact the radiation budget (Section I.15), with consequences for evaporation and regional climate that are not yet quantified.

Finally, Section I.16 discusses the climate projections that are an attempt to establish possible future climate scenarios in the Mediterranean region and their uncertainty. Section I.17 discusses the most relevant issues with regard to the main objectives of present climate research.

I.2 Socioeconomic Characteristics and Main Vulnerabilities

The Mediterranean basin is characterized by strong socioeconomic differences, in particular, between the northern Mediterranean countries (NMCs) and the southern and eastern Mediterranean countries (SEMCs). Though the situation is changing rapidly, and the SEMCs are increasing their annual primary energy demand at more than 4% per year, at present, the NMCs have about a four times higher per capita gross domestic product than the SEMCs, a three times higher per capita energy supply, more than twice as high per capita CO_2 emissions, and four times more tourist arrivals, with the Mediterranean accounting for 30% of the world's international tourism (Plan Bleu, 2009).

While population development in the north is almost stagnant, strong population growth in the southeast (in combination with a lack of effective policies) results in overexploitation of water, land, and other resources, driven by land clearing, cultivation of marginal land, overgrazing, and firewood harvesting. Currently, 80% of all dry lands in the SEMCs are affected by desertification (Plan Bleu, 2005). Land productivity is decreasing accordingly. In contrast, many rural areas in the NMC experience abandonment of agricultural land, with subsequent encroachment of shrubs and trees and a greening of the land. Forest cover in the NMCs is much higher than in the SEMCs. The SEMCs are rapidly urbanizing—with almost all of the future population growth projected to be in the cities—while urbanization rates in the north are more or less stable (Plan Bleu, 2005).

Precipitation in the Mediterranean in unevenly distributed (see also Section I.6), being scarce and irregular in many southern areas, where water availability is already a problem. There is a significant risk of reaching climate conditions (see Section I.15 and Chapter 8) that will imply a much drier state of the land and atmosphere than at present. Likely, the simultaneous action on the environment of climate and other anthropic factors (such as deforestation, draining of wetlands, and adoption of water-saving technologies in irrigation) will produce further land degradation, to which the Mediterranean social-ecological systems seem to be quite vulnerable.

Per capita water availability in the NMCs is three times higher than in the SEMCs. Water scarcity in the south is compounded by higher loss rates and lower water productivity in all sectors. The gap between water availability and demand is currently widening further in the south because of rapid population growth and is projected to become even wider in the future because of conditions becoming progressively drier than in the north with climate change. Irrigation accounts for 40% (80%) of total water demand in the NMCs (the SEMCs). While irrigation is primarily an adaptation strategy to climate variability, the growing dependence on irrigation in the Mediterranean is likely to increase economic and social vulnerability further, given projections of reduced total water availability and rapidly growing competing urban water demands. An indication for water-quality problems is the fact that 10% (50%) of the cities and 5% (20%) of population in the NMCs (the SEMCs) are not connected to any wastewater treatment (Plan Bleu, 2005, 2009).

Agricultural (water) productivity is low in most SEMCs, with frequent crop failure due to droughts. Yield increases have remained below the world average over the past few decades, aggravating the problems due to higher climate variability and lower per capita water availability as compared with the NMCs. Cultivation of more marginal land and urbanization (often resulting in a loss of the most productive agricultural land) further suppress agricultural productivity in the south. north African countries have already experienced a sharp decline in per capita rain-fed agricultural production in years (IAASTD, 2008). As a result (also in response to the overuse and depletion of groundwater), SEMCs have become net importers of virtual water (Yang et al., 2007; Fernandez and ENGREF, 2007). Their dependence on virtual water imports is growing rapidly, already being higher than in any other region of the world. Net virtual water imports in several SEMCs are approaching or even exceeding the renewable blue water resources. This situation makes them increasingly vulnerable to price hikes in international markets.

All of these factors in combination indicate a higher vulnerability to climate change of the SEMCs, given the lower adaptive capacity and at the same time higher exposure to droughts and desertification as compared with NMCs. SEMC economies, employment, and livelihoods depend more strongly on agriculture and hence on water resources and climate. Greater climate-change impacts in the south are met by a lack of technical, financial, and institutional means to implement climate adaptation solutions on a large scale. With respect to the NMCs, SEMCs generally have lower literacy rates and rank lower on indexes of good governance, democracy, and corruption.

Beyond the north–south gradient in the Mediterranean, particularly vulnerable landscapes include deltas and coastal zones (vulnerable to sea-level rise), as well as rapidly growing cities without adequate infrastructure and institutions. In the Mediterranean region, 50% of the urban population lives less than 10 m above sea level (Plan Bleu, 2005, 2009). Tourist destinations (concentrated along the coast) are vulnerable not only to sea-level rise but also to higher summer temperatures, which may turn tourists away toward more northern and cooler locations.

I.3 The Mediterranean Region

The characterization of the region is strongly linked to the Mediterranean Sea, a semi-enclosed, mostly deep regional sea. Its presence is, however, not sufficient for determining a uniform climate. Strong contrasts among different areas are present, deriving from the complicated morphology of the Mediterranean region and its location between the subtropical zone to the south and the temperate zone to the north. According to the traditional climate classification (Köppen, 1900) the Mediterranean climate is defined as a midlatitude temperate climate with a dry summer season, which can be either warm or hot (these two types are labeled Csa and Csb, respectively, in the Köppen classification). However, the Csa and Csb classifications apply only to a fraction of the Mediterranean region (Figure I.1). The distance between most parts of this region and the sea is only a couple hundred kilometers; however, other temperate, arid, and snow climate types are present. The contrasts are large: There are permanent glaciers in the humid alpine area north of the Mediterranean Sea and hot subtropical desert areas at the southern African coast, a temperate maritime climate at the north Iberian coast west of the Mediterranean Sea and truly Mediterranean areas, and steppe in the Middle East regions at the eastern coast. Note also the large areas with midlatitude temperate climate and with no dry summer (Cfa and Cfb) in the northern parts of the Mediterranean. The mean annual cycles of the climate types that are present in Figure I.1 are shown in Figure I.2, which shows the

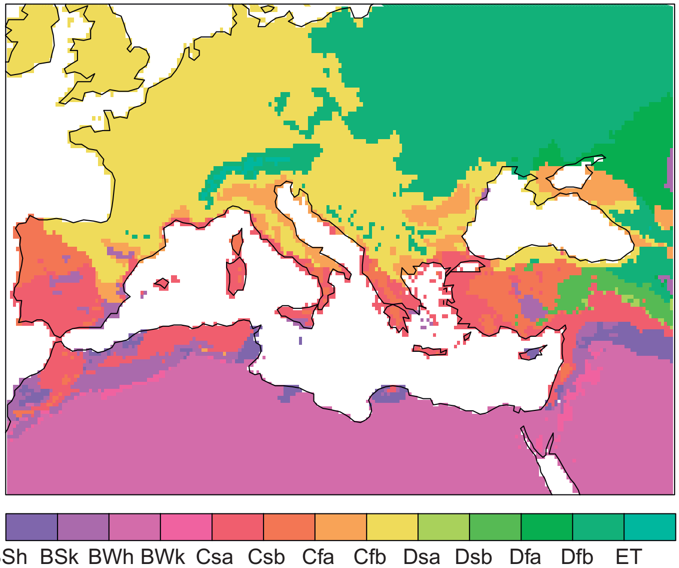

Figure I.1 Köppen climate types in the Mediterranean region: subtropical steppe (BSh), midlatitude steppe (BSk), subtropical desert (BWh), midlatitude desert (BWk), Mediterranean climate with hot/warm summer (Csa/b), humid subtropical with no dry season (Cfa), maritime temperate (Cfb), humid continental with hot/warm summer (Dfa/b), continental with dry hot/warm summer (Dsa/b), and tundra (ET). This figure is based on Climatic Research Unit (CRU) temperature and precipitation gridded data (New et al., 2000).

large range of temperatures and the different behavior of precipitation among the different zones. Note the scarcity of summer precipitation in many areas.

The location of the Mediterranean region in a transitional zone between subtropical and midlatitude regimes (for a review, see Lionello et al., 2006a; Alpert et al., 2006a; Trigo et al., 2006) is another important factor of space and time variability. In general terms, there is a difference between the northwestern and southeastern areas, though this cannot be considered a rigorous distinction. The northern part of the region is strongly linked to the midlatitude variability, characterized by the NAO (north Atlantic oscillation) and other midlatitude teleconnection patterns (Xoplaki, 2002; Dünkeloh and Jacobeit, 2003; Xoplaki et al., 2003, 2004; Lionello and Galati, 2008; and Chapter 3). Different from areas in northern Europe or along the European Atlantic coast, many northern hemisphere teleconnection patterns besides the NAO exert a comparable influence on regional variables, such as the Scandinavian Pattern, the East Atlantic, and the East Atlantic/northern Russia pattern (Xoplaki, 2002; Lionello and Galati, 2008; and Chapters 5 and 6). The consequence is that many patterns need to be included for describing a significant fraction of climate variability. The southern part of the region is under the influence of the descending branch of the Hadley cell for a large part of the year and is exposed to the Asian monsoon in summer. The effect of the El Niño Southern Oscillation (ENSO) has been detected

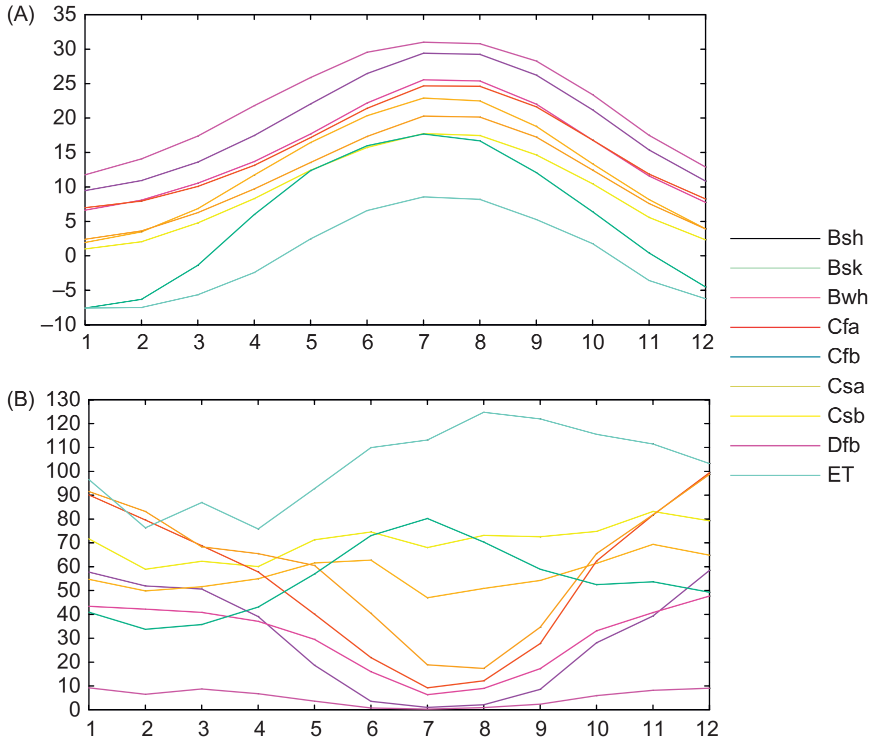

Figure I.2 Mean annual cycles of temperature (A, monthly average temperature, °C) and precipitation (B, mm/month) of the Köppen climate types in the Mediterranean. Each line corresponds to the spatial mean over the corresponding areas in Figure I.1. Data and labels used are the same as in Figure I.1.

mainly on precipitation, and it is variable in time but not negligible (Mariotti et al., 2002a; Alpert et al., 2006a). This northwest (midlatitude influences) versus southeast (subtropical influences) separation allows for many exceptions, such as the effect of ENSO on autumn precipitation in the northwestern Mediterranean region (Knippertz et al., 2003) and the effect of northern hemisphere patterns such as NAO on Middle East precipitation (Alpert et al., 2006b).

The complicated land–sea pattern—with many islands of various sizes and peninsulas dividing the Mediterranean Sea into many subbasins connected by narrow straits and the presence of steep mountain ridges close to the coast—helps to explain the spatial heterogeneity of climate in the Mediterranean region (as shown in Figure I.1) and represent a well-known problem for the correct simulation of its climate. The effect of the mesoscale morphological features on atmospheric circulation and air–sea and land–atmosphere interaction and the constraints they pose on sea circulation are crucial for an adequate simulation of Mediterranean climate (Lionello et al., 2006a,b). All these morphological factors need high resolution to

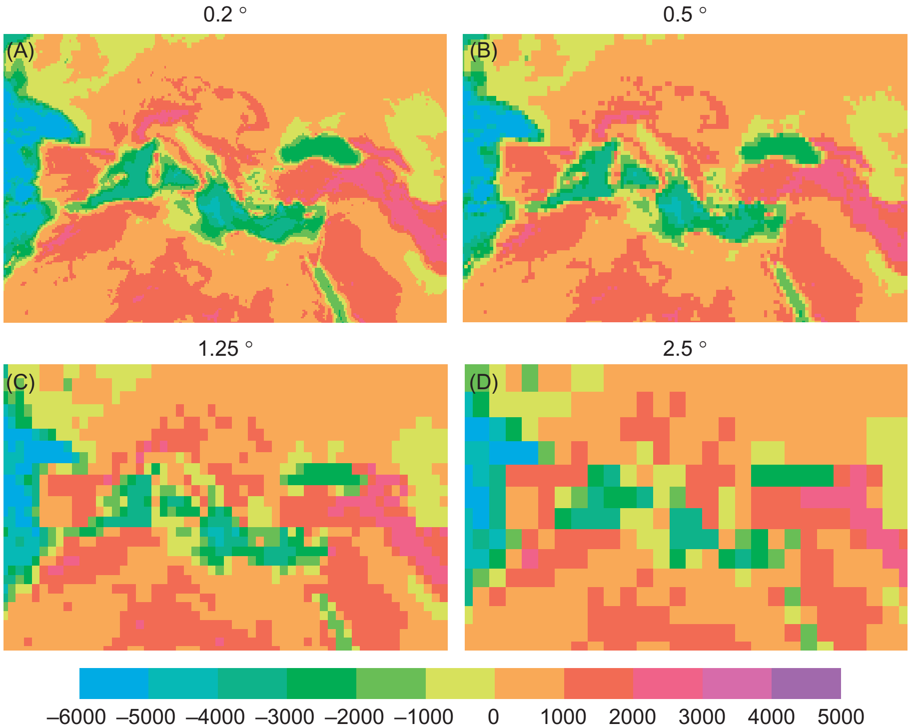

Figure I.3 Representation of bathymetry and topography of the Mediterranean region aggregating data in cells of increasing size: (A) 0.2°, (B) 0.5°, (C) 1.25°, and (D) 2.5°.

be accounted for in numerical simulations, and this requirement has been for a long time beyond the capabilities of climate models and computers. Figure I.3 shows the representation of bathymetry and topography aggregating data in cells of various size. Approximately, Figure I.3A corresponds to the resolution recently achieved by RCMs (Regional Climate Models) and Figure I.3D corresponds to the average resolution of the global models used in the Intergovernmental Panel on Climate Change 4th Assessment Report (IPCC AR4) and in the analysis by Giorgi and Lionello (2008). The two remaining panels correspond to the resolution of two widely used data sets in climate research: the ERA40 reanalysis data set (Figure I.3B; Uppala et al., 2005) and the CRU (Climatic Research Unit) gridded climatology (Figure I.3C) (New et al., 1999). The more recent E-OBS data set (Haylock et al., 2008) based on gridded station data has a resolution comparable to that shown in Figure I.3A. It is clear that only Figure I.3A and B can be considered adequate for representing realistically the morphology of the region, and even a model working at these high resolutions is far from being adequate for simulating hydrological processes in narrow and steep basins of the Mediterranean region. For precipitation, a field with high spatial variability, the resolution required for producing reasonably accurate simulations of the hydrology is discouragingly high. It can be shown that the ratio between precipitation field resolution and size of the hydrological basin should be less than 0.2 for obtaining a reasonably small error of river runoff, implying a 2 km resolution for a river basin with an area of 100 km^2 (Sangati and Borga, 2009).

I.4 Paleoclimate Reconstruction

Paleoclimate records indicate that climate has varied throughout geological time at different timescales, from millions of years (My) to annual or even seasonal scales. Reconstructions of climate variability on geological timescales are based on the study of "climate archives" that contain information on climate variables (e.g., temperature, precipitation, and wind) and that extend our understanding of climate far beyond both the approximately 150 years of instrumental records and the 4.5 millennia of historical records. Some climate archives, such as sediment sequences on land or from shallow ocean areas, can provide information dating back millions of years but are mostly limited to specific time windows. Other climate archives, such as tree rings, ice cores, corals, speleothems, lake sediments, and deep-sea sediments, allow us to obtain information from multidecadal to hundred thousands to millions of years—either as short glimpses in time (e.g., life span of a tree or coral) or as continuous records.

Past-climate reconstruction draws upon the knowledge of modern oceanography and climatology. Reconstructions of parameters such as air temperature, precipitation, wind, sea-surface temperature (SST), and ocean salinity at any place and time in the past are interpreted, if possible, in the context of the relevant physical and dynamical processes (e.g., ocean or atmospheric circulation patterns) known to be operating within the climate system. However, given that past-climate variables cannot be directly measured, information is derived through the use of proxies. (A proxy is any component of a climate archive whose origin is related to a climate variable or process and whose relationship holds for a wide variety of oceanographic and sedimentological environments and timescales.) Reviews of existing proxies for various climate variables, including thoughtful evaluations of the problems and difficulties associated with the measurements and/or use of each of them, have been published by Abrantes and Mix (1999), Fischer and Wefer (1999), Hillaire-Marcel and De Vernal (2007), and Ruddiman (2007).

For the reconstruction of oceanographic conditions, with regard to circulation, chemistry, biology, and patterns of sedimentation, there exist different types of proxies. A great majority of them are related to the biogenic component of deep-ocean sediments. These proxies are typically microorganisms (phytoplankton and zooplankton) that lived in the ocean throughout geologic times and synthesized a fossilizable shell or internal skeleton. The small size of these shells/skeletons means that even a small sediment sample contains a large number of them, such that it permits a statistically reliable data set. The organisms' abundance and assemblage's composition give important information on past SSTs, relative salinity, and nutrient and water-column conditions. Geochemical proxies such as stable and unstable isotopes, major and minor sediment components (e.g., carbonate, opal, major, minor, and trace elements in microfossil shells and sediments) are also very important in learning more about the dynamics of the carbon and nutrient cycles.

For the past 800 thousand years (ky) (associated with the so-called orbital-to-millennial scale variability) air-temperature reconstructions typically come from ice cores (Jouzel et al., 2007). For other archives, estimations are based on the types of fossil organisms found at any one time and location. The same is also true for precipitation, which is estimated mainly from fossil organisms, pollen, lake levels, speleothems, and sediments' geochemical components, except for more recent periods (e.g., the historical period), for which quantitative precipitation estimates are possible from tree rings. Most of these estimates are of a qualitative or semiquantitative nature. However, laboratory experiments, combined with a comparison of spatial data sets to modern climate and/or environmental variables, allow for a better quantitative reconstruction. Despite this, the uncertainty of such quantifications can be difficult to assess, since it would require the replication of paleorecords, which has generally been economically impossible. Furthermore, each proxy is subject to a unique combination of uncertainties that are generally difficult to identify, and the assumption that relationships between variables do not change over time and under varying climate forcing is a source of uncertainty in itself. One method to reduce this type of uncertainty is known as the "multiproxy" approach—i.e., the use of a combination of plausible proxies in order to minimize the ambiguity and maximize the accuracy of any estimation. Even in these cases, timescale uncertainty remains a source of error in climate reconstructions and age determination is fundamental, with any record being only as good as its age model. The available dating methods (e.g., radiogenic isotopes and magnetic patterns on the seafloor and in sediments) or even varve counting in ice cores or laminated lake records have associated errors, which are imposed on the dated archive.

The evolution of the Mediterranean Sea and the southwestern Portuguese region are extensively discussed in Chapter 1. Morphologically, the Mediterranean Sea became an isolated basin approximately 11 My ago, when it was separated from the Indian Ocean, to which it had previously been connected through a large and deep passage located along the present southern Turkey and Iraq. The Mediterranean region was (and remains) tectonically very active, and the successive restriction and finally complete closure of the gateways between the Mediterranean Sea and the Atlantic Ocean between 7 and 5.33 My ago resulted in the desiccation of the basin and a "salinity crisis," during which the Mediterranean Sea's salinity reached extremely high values ($>$49 psu) and the sea level at some point dropped at least 1500 m below its present level. The opening of the Strait of Gibraltar 5.33 My ago abruptly ended the salinity crisis and resulted in a rapid sea-level rise to the Atlantic Ocean's level. This event can be considered as marking the birth of the Mediterranean environment as we know it today, though, obviously, the climate has been far from constant since then. With the onset of the northern hemisphere glaciations about 2.7 My ago, the Mediterranean region started to experience climatic changes on glacial/interglacial cycles. Interglacials, and other periods associated with high insolation, were characterized by episodes of anoxic conditions linked to the monsoon cycles and subsequent increased freshwater fluxes that caused high stratification in the upper MW and the collapse of the subsurface ventilation. The timing and duration of these episodes varied across the basin. For an anoxic period that took place around 122 ky BP (Before Present) ago, i.e., during the last interglacial, the collapse of the subsurface ventilation occurred within 40–300 years, depending on location, and lasted approximately 600–900 years. Climate conditions during different interglacial periods were not exactly the same. The last interglacial (128–110 ky BP), for example, was warmer and more humid than the present interglacial, the Holocene, in most of the Mediterranean region. After the last deglaciation, relatively stable conditions have persisted for the past 11 ky BP (i.e., the Holocene) and are characterized by an overall trend from initially warmer and wetter conditions to the present climate, with a dry period that initiated about 5.5 ky BP ago and continues now.

I.5 The Climate of the Mediterranean Region in Historical Times

A peculiarity of the Mediterranean region is the strong anthropic action on the environment exerted over several thousand years. Since the onset of the earlier civilizations in this region, humans have strongly influenced and modified the Mediterranean environment to such an extent that their impact may obscure the climatic signal, mainly regarding vegetation, forest, and fire regimes. Land use, for instance, is a significant parameter for modifying regional climate in the Mediterranean, and it is an extremely important indicator of changing environments and landscapes (Reale and Shukla, 2000; Carrion et al., 2010; Zampieri and Lionello, 2011).

The Mediterranean offers a variety of natural archives and historical written information. Combining information from the different archives with evidence of past human activity obtained from paleoecological, historical, and archeological records helps to advance our understanding of the climatic sensitivity, environmental response, ecological processes, and human impact down to the regional scale.

The currently available data not only provide a rough idea of the potential of climate proxies to reconstruct climate variations at the local scale but also stress limitations to sufficiently reconstruct the full range of natural climate variability, including interannual to multicentennial variations. Our understanding of variations in paleohydroclimatic changes across the Mediterranean is still limited because the limited number of well-dated high-temporal-resolution proxies that resolve different seasons are unevenly distributed over the area. Furthermore, the identification and characterization of past extreme events (e.g., the onset, duration, frequency, and intensity of droughts and floods) can be derived only for particular areas and time periods.

The evidence presented in Chapter 2 shows that the climate over the Mediterranean during the past 2000 years has experienced a sequence of humid/dry and warm/cold periods that have produced effects on environmental conditions (Colombaroli et al., 2007; Carrion et al., 2010). A currently available reconstruction covering the entire land areas for winter during the past 500 years suggests variability in the range of 0.5 K for temperature and 20 mm for precipitation, when these quantities are averaged over the whole Mediterranean region and over decadal timescales (Luterbacher et al., 2006). However, these are very conservative estimates, because the combination of the statistical method and the scarce information available determines a systematic underestimation of the true values, which can be very large for precipitation and the reconstruction of a consistent regional scale evolution from local records is not completed yet.

Two main periods identified in the recent climate evolution are the Medieval Climate Anomaly (MCA) and the Little Ice Age (LIA) (Mann et al., 2009; Luterbacher et al., 2012). The LIA is conventionally defined as a cold period extending from the sixteenth (initial date is controversial) to the nineteenth centuries, which in Europe was characterized as a period of glacier expansion in alpine regions—recorded not only in glacial features dated by geologic techniques but also in historical documents, such as field sketches, land values, and weather records. The MCA denotes a period from the tenth to the fourteenth century when evidence suggests that Europe, Greenland, and Asia experienced relative warmth. Global extension and timing of both the MCA and the LIA are, anyway, controversial (Bradley et al., 2003; Xoplaki et al., 2011, and the references therein). Lake sediments suggest that in the Pyrenees, the warmest winters occurred during the MCA and also in the Roman Warm Period (2.7–2.4 ka BP), and around AD 450, and winters were the coldest during parts of the LIA (mainly at the end of the seventeenth century), but also in the period AD 1050–1175. Lake-level evidence from the Pyrenees also indicates a drier and warmer MCA and generally wetter and colder conditions during the period AD 1400–1850. Tree-ring data suggest that summer temperatures in the Pyrenees were warm during the fourteenth and fifteenth centuries and within the twentieth century, separated by a prolonged cooling during the LIA. In Spain, pollen and sedimentological data indicate another arid period between AD 700 and 1400 synchronous with the MCA and two humid periods—AD 1200–1400 and approximately AD 1600, i.e., during the LIA (Roberts et al., 2011 and the references therein). Tree-ring data from Morocco point to a drier MCA and a wetter LIA (Esper et al., 2007). However, characterizations of the LIA and MCA are not uniform across the Mediterranean: lake sequences from central Anatolia (Turkey) during the past 1200 years show a reverse pattern, with wetter (drier) conditions during the MCA (LIA) (Roberts et al., 2011 and the references therein). Moreover, variability is not restricted to the LIA and MCA. Varve-based evidence from the Pyrenees shows that the most humid period during the past 4 ka occurred during the Iberian and Roman ages (2.5–1.6 ka BP, 550 BC to AD 350), but included a relatively arid interval during the Roman Imperial Epoch (190 BC to AD 150).

For precipitation, the large variability at many timescales prevents drawing any conclusion; however, data available at present from a limited number of proxies provide no evidence in the past of a fast temperature increase in the Mediterranean such as that observed in the last decades of the twentieth century. Chapter 2 provides an extensive discussion and bibliographic references on climate variations during historical time in the Mediterranean.

I.6 Present Seasonal Temperature and Precipitation and Their Trends

The knowledge of present climate conditions is different from that of the past periods considered in the two previous sections, because it can rely on instrumental time series. However, this is not free from problems, because information is often too sparse in space and irregular in time. Considering the Mediterranean region, meteorological stations with long reliable time series are not uniformly distributed, and there is a strong contrast among different areas on the density of data and periods covered. Usually, there are more records available in public archives from northwestern areas than from the rest, with northern Africa having very far from adequate coverage with sufficiently long time series (New et al., 1999; Haylock et al., 2008). In order to be used for regional-scale climate analysis, observed data need to be transferred to regular grids and statistical methods used to compensate for the variable density of the meteorological stations and for periods with no data in the single time series. The results are gridded data sets that are, on the basis of the available information, optimally homogeneous in the quality of the time and space coverage (New et al., 1999; Haylock et al., 2008).

Seasonal values of average temperature and accumulated precipitation of the CRU data sets at 0.5° resolution (New et al., 2000) are shown in Figure I.4. The panels represent the average values for the period 1961–1990. The background meridional temperature gradient is altered by the effects of orography and complicated land–sea patterns. The main mountain ridges (Pyrenees, Alps, Atlas, Balkans, and Anatolians) determine a cool signature in all seasons. With the exception of some mountain areas, summer is warm or hot in the whole region. In general, July is the warmest month, with average maximum temperatures above 35°C in many locations (e.g., Jendouba, Gabes, and Kebili in Tunisia; Taroudant in Morocco) (Dubief, 1959). Subregional features tend to dominate the spatial distribution of precipitation, which broadly decreases from wet areas in the northwest to arid and semi-arid areas in the southeast. Mountain ridges are evidently associated with local precipitation maxima connected with orographic precipitation. The dominant eastward atmospheric circulation, which transports the moisture from the Atlantic and the Mediterranean Sea itself toward the coasts, is responsible for the maxima especially along the western coasts of peninsulas and main islands. Note that summer is generally drier than the rest of the year over most of the Mediterranean region. A notable exception is the Alpine region, where precipitation actually has a maximum in summer.

Figure I.5 shows precipitation over the sea. It is based on the CMAP data set (Xie and Arkin, 1996, 1997) and covers the period 1979–2002, at a 1° resolution. Since over sea *in situ* observations are too sparse and infrequent, satellite observations are an essential source of information for the reconstruction of precipitation patterns. Data in Figure I.5 are produced using a technique that merges observations from rain gauges with precipitation estimates from several satellite-based algorithms. The large annual cycle, with hardly any precipitation in summer, and the precipitation gradient, with values decreasing toward the south, are features common to both

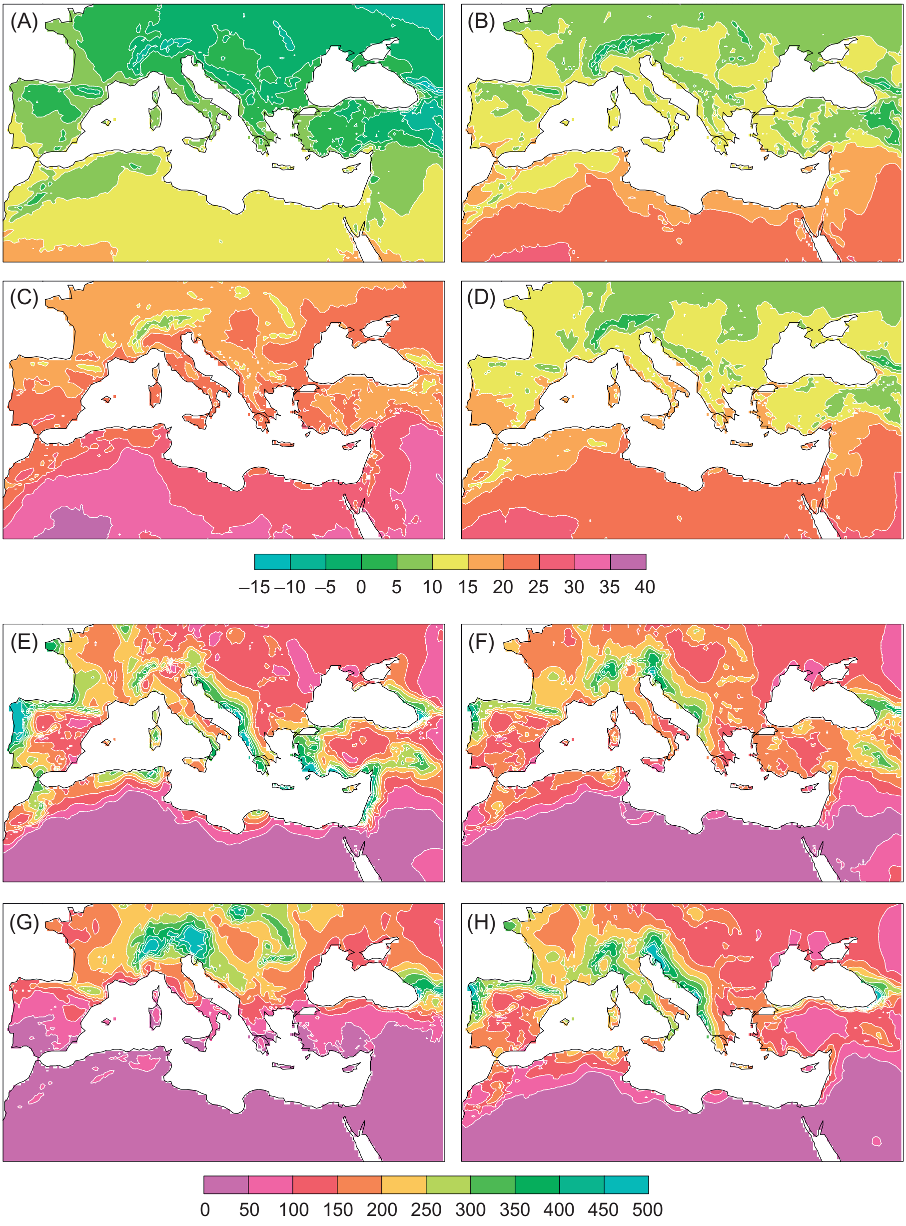

Figure I.4 Seasonal (winter: December–January–February; spring: March–April–May; summer: June–July–August; autumn: September–October–November) mean temperature (°C, panels A–D) and total precipitation (mm per season, panels E–H) maps for the period 1961–1990 based on CRU data.

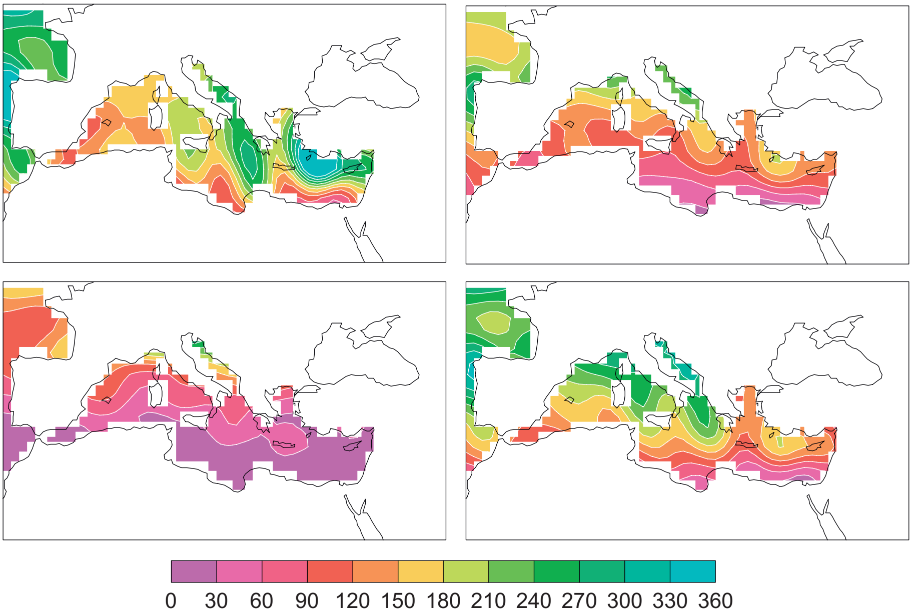

Figure I.5 Total seasonal precipitation over sea (mm per season) for the period 1979–2002. Plots are based on the CMAP data set at 1° resolution.

sea (Figure I.5) and land (Figure I.4) data. In general, precipitation maxima are lower over sea than over land. Maxima are located at the southern coast of Turkey (winter), in the Gulf of Lions (autumn), and in the Ionian Sea, which is characterized by a large meridional band whose amplitude has maximum in winter and disappears in summer.

Figure I.6 shows the present rate of change of the temperature (°C per decade) and precipitation (mm per decade), seasonal climatologies that are shown in Figure I.4. Figure I.6 is based on CRU data (New et al., 2000) and refers to the period 1951–2005. Only areas where trends are significant at the 90% confidence level are plotted. All statistically significant temperature trends are positive. Trends are particularly large in summer over the whole western Mediterranean and in spring in its central part. The warming shown in these figures is consistent with many analyses that have been carried out at subregional scales, using direct station data. The situation is less unequivocal for precipitation, whose intrinsic and high interannual variability prevents the identification of significant trends over large areas. The main observed feature for precipitation is its winter decrease over small areas in the Balkan and Italian peninsulas, in the southern Anatolian coast, and in a part of northwest Africa. Also, these features are confirmed by several studies based directly on station data (Xoplaki, 2002).

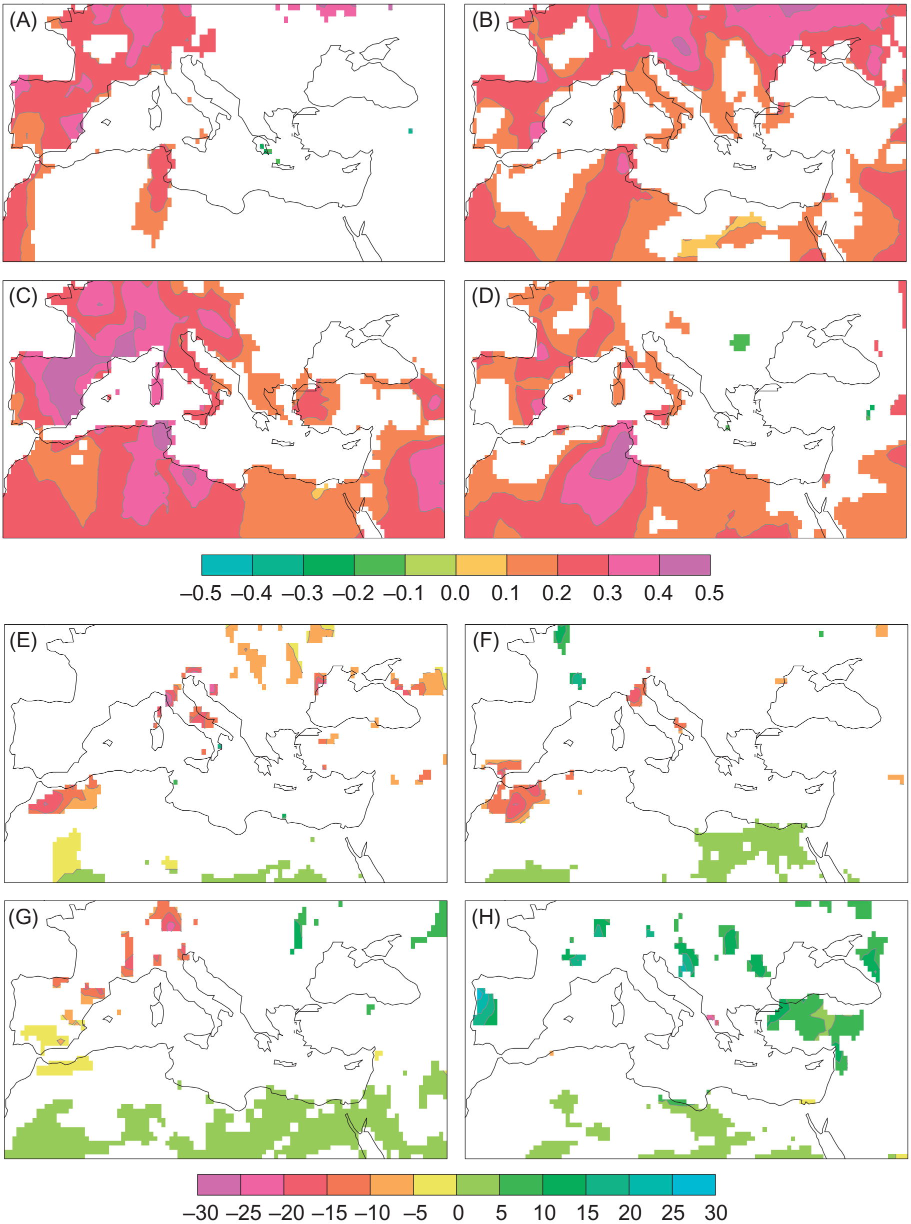

Figure I.6 Trends of the seasonal (winter: December–January–February; spring: March–April–May; summer: June–July–August; autumn: September–October–November) mean temperature (°C per decade, panels A–D) and total precipitation (mm per decade, panels E–H) for the period 1951–2005 based on CRU data. Only significant trends at the 90% level are plotted.

I.7 Rain Spells and Their Characterization

The proximity to three continents, the complexity of the morphology of the area, the significant effects of local factors, and the prominent influence of various teleconnection patterns (see also Chapter 5) determine in this region the presence of significant differences in the total precipitation (computed both on seasonal and on annual bases) and in the distribution of daily precipitation. The total annual precipitation in the Mediterranean region varies between values greater than 1200 (mainly along the eastern coasts of the Adriatic) and less than 400 mm (mainly along the north African coasts and the southeast Mediterranean). Furthermore, the same total annual precipitation may be obtained by quite different daily distributions.

The number of rain spells (NRS), the rain-spell yields (RSYs), and the rain-spell duration (RSD) are examples of parameters that characterize the precipitation in the Mediterranean region. A rain-spell is a period of consecutive days with rainfall above a fixed daily rainfall threshold (DRT), and RSY is the total amount of precipitation during a rain spell. Reiser and Kutiel (2010b) proposed to select for each station a DRT such that all small events contributing together the lowest 4% of the total annual precipitation are omitted. This choice causes a decrease of the NRS, typically ranging between 5% (e.g., southwestern France) and over 30% (e.g., eastern Spain). Figure I.7 illustrates the relationship between total annual precipitation, NRS, and RSY in 41 Mediterranean stations. Each station is represented by a dot located at the

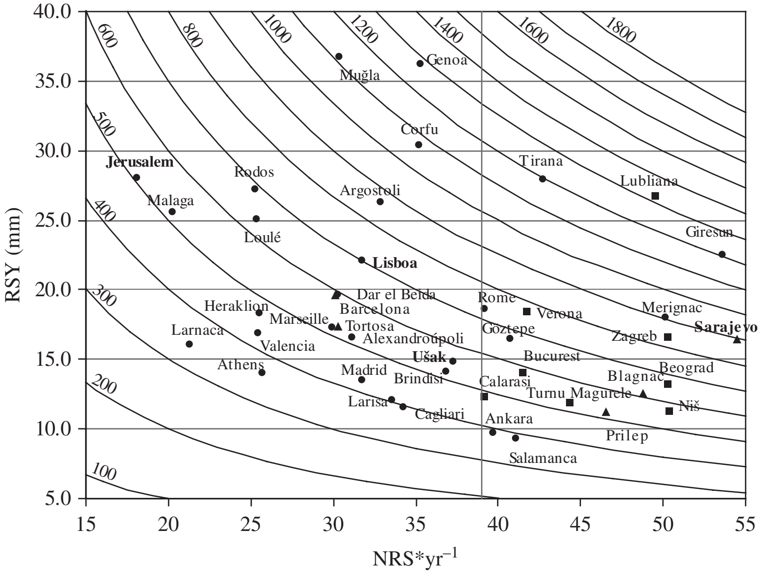

Figure I.7 Relationship between average NRS and average RSY.
Source: Adapted from Reiser and Kutiel (2010b).

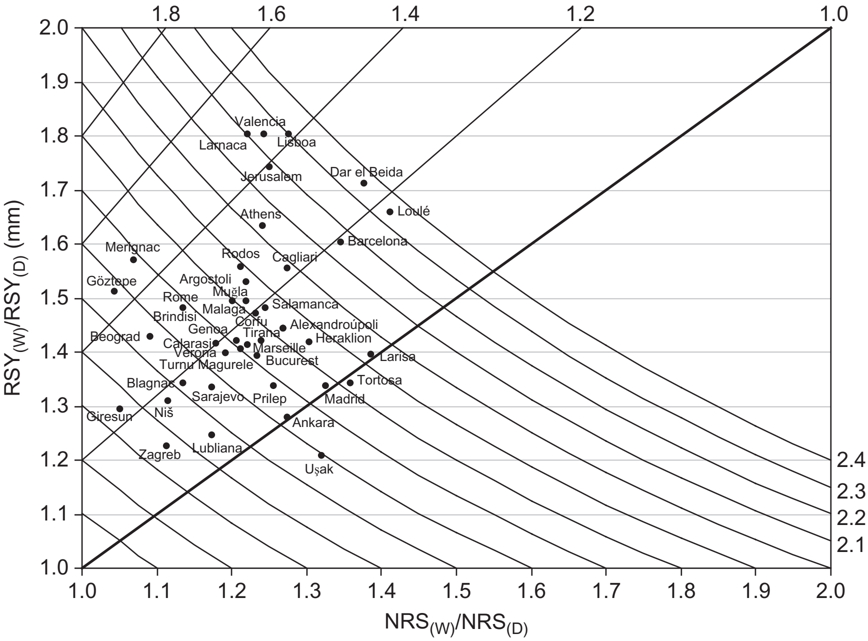

Figure I.8 Relationship between the ratios in dry and wet seasons for NRS and for RSY. Oblique lines show RNY and curved lines represent RWD.
Source: Adapted from Reiser and Kutiel (2010b).

intersection of the average annual NRS and the average RSY. The curved lines represent the total annual precipitation. Stations with very similar annual totals can greatly differ in their NRS and RSY—e.g., Tirana and Giresun or Blagnac and Dar el Beida.

A rainy/dry year may result from an increase/decrease in the NRS, the RSY, or both. Figure I.8 illustrates this difference. A year is defined to be dry (wet) when its total precipitation is half a standard deviation below (above) the long-term station average. The respective dry-year and wet-year totals are denoted as TOTAL(D) and TOTAL(W), respectively. Similarly, one has NRS(D) and NRS(W). The wet:dry ratio (RWD) between TOTAL(W) and TOTAL(D) and the number-yield rain-spell ratio (RNY) between NRS(D) and NRS(W) are used for the characterization of the precipitation regime in each location. The oblique lines represent the RSY:RNY ratio. Values greater than 1.0 (above the central line) mean that the RSY is more important in causing a year to be wet or dry. The opposite is true with values less than 1.0 (below the central line), where the NRS is the key factor. Note that a great majority of the stations (and this is more evident in the southern Mediterranean) are located above this central line, meaning that mostly the average yield of the rain spells (and not the number of events) is the factor causing the difference of total precipitation between rainy and dry years.

Note that the list of parameters discussed in this section is very limited. The dry days since last rain (Aviad et al., 2007) and rainy season length and the date of different accumulated percentage (Paz and Kutiel, 2003, Reiser and Kutiel, 2010a) are examples of interesting quantities that are not considered here and are very useful for describing the rainfall distribution within the rainy season.

I.8 Temperature and Precipitation Extremes

Though mean values are a main parameter describing a statistical distribution (and it is the unique parameter taken into account in many studies), the likelihood of large deviations from the mean is of paramount importance for many environmental applications. The probability of large deviations generally decreases with their size and is associated with the variance of the distribution and its higher moments. Such large deviations represent extreme values, which happen rarely and are associated with hazardous situations: anomalously high/low temperatures are associated with heat waves/cold spells, high precipitation to floods, and lack of precipitation to droughts, for instance. The analysis of the probability of occurrence of extremes presents difficulties, which are mainly related to the insufficient availability of long time series of quality controlled data for a robust assessment of their statistical distribution. Daily, or optimally hourly, resolution is needed to estimate many extremes, such as daily temperature maxima and intense precipitation events. Estimates of extremes values is necessarily based on few events whose occurrence is highly irregular in space and time and is therefore characterized by a larger uncertainty with respect to mean values.

Often research of extremes, because of the above reasons, cannot be focused on events with a return time of several decades and is therefore limited to the study of moderate extremes that are defined by high/low percentiles (usually in the range of the 90th to 99th percentiles) of the statistical distribution for which much more data are available. All these issues are of particular relevance for the Mediterranean region, where droughts, heat waves, and floods (events of small spatial scale) are risks that environment and societies in the area have always faced and whose intensity may change in the frame of climate change (see also Chapters 5, 6, and 8).

I.8.1 Temperature Extremes

Daily data for the computation of trends in Mediterranean temperature extremes over the past 50 years (1958–2008) are provided by gridded station data (E-OBS data set) (Haylock et al., 2008) and ERA40 meteorological reanalysis data (Figure I.9; Efthymiadis et al., 2010). Results are consistent with the global picture of a warming world (Alexander et al., 2006).

The agreement of observed changes in the Mediterranean with global-scale warming is most evident in summer (Figure I.9B), when the number of very hot days (denoted as TX95N, days with maximum temperature exceeding the local 95th percentile) has increased significantly across the basin and the number of very cold nights (TN5N, nights with minimum temperature below the local 5th percentile) has

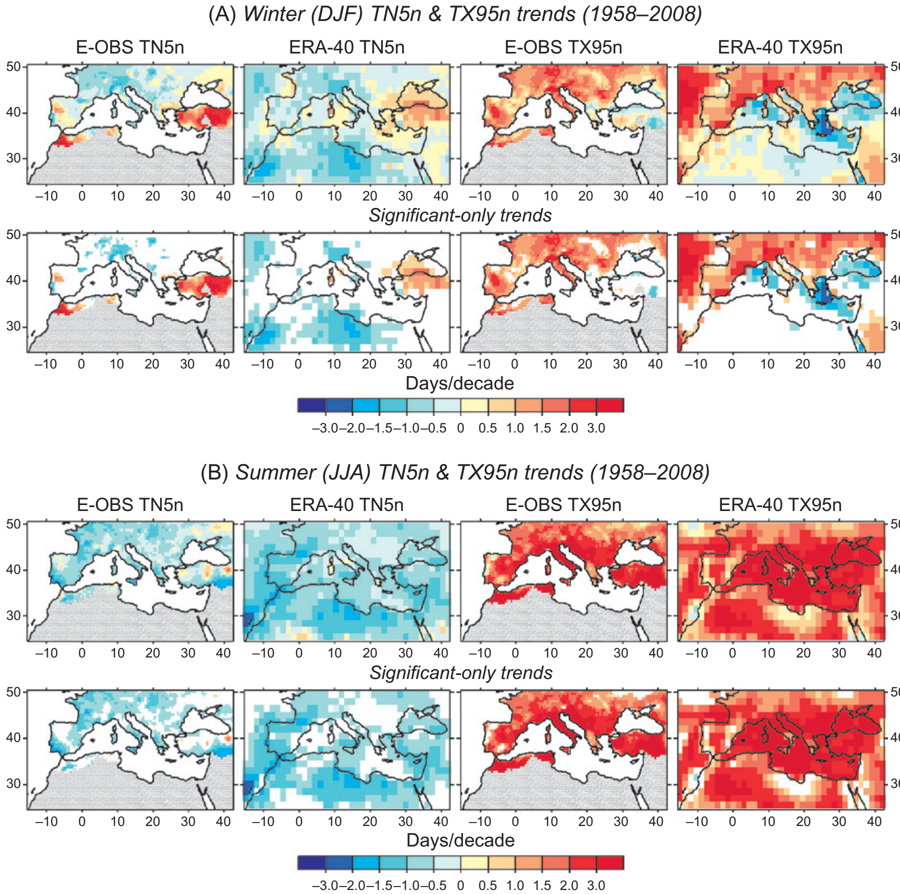

Figure I.9 Trends in indexes of temperature extremes (very cold nights (TN5N) and very hot days (TX95N)) over the period 1958–2008 calculated from gridded station (E-OBS, land only) and ERA40 reanalysis data. All trends are shown in the upper panels, while only statistically significant (at the 5% level) trends are shown in the lower panels. Units are days per decade. (A) Winter; (B) summer.

decreased everywhere (significantly so in most land areas). Over the Mediterranean Sea itself, Italy, and parts of the eastern Mediterranean and north Africa, the rate of increase in very hot days is more than 3 days per decade. In contrast, the rate of decrease in very cold nights tends to be somewhat smaller (up to 1–2 days per decade) over land and smallest over the Mediterranean Sea.

In winter (Figure I.9A), the number of very cold nights tends to decrease and the number of very hot days tends to increase. The pattern of warming is, however, less uniform than in summer and the trends are weaker (up to 2–3 days per decade in the case of very hot days) and statistically significant over a smaller area. While the main pattern is one of warming, there are some spatially coherent exceptions. In particular, the number of cold nights increases in the eastern Mediterranean over the Aegean and Black Seas and Turkey by up to 2–3 days per decade and also over parts of northwest Africa. There is also a decrease in the frequency of very hot days in these eastern Mediterranean areas—strongest over the Aegean.

The similarity of the trends over land in both data sets, together with the large and coherent areas of statistically significant trends, indicates that they are quite robust. By definition, there are on average 4.5 very hot or very cold days each season averaged over the period 1961–1990; thus, increases at rates of 2–3 days per decade are quite substantial. Similar trends are also seen in other indexes of temperature extremes calculated from these data sets (Efthymiadis et al., 2010; García-Herrera et al., 2011). In particular, summer heat waves have become markedly longer over sea (increasing at a rate of >1.5 days per decade) and moderately longer over land areas surrounding the basin (a maximum of 1–1.5 days per decade over northern Italy). Increases in the number, intensity, and length of heat waves have also be found for the eastern Mediterranean basin based on long, homogenized station time series (Kuglitsch et al., 2010).

I.8.2 Precipitation Extremes

Mediterranean precipitation extremes make an important contribution to the seasonal totals. Approximately 60% of the total is attributed to precipitation extremes—i.e., events above a high station-based threshold (Toreti et al., 2010).

The analysis of extreme precipitation in the Mediterranean is based on 286 stations across the basin for the period 1950–2006. The extended winter/wet period for the Mediterranean (Xoplaki, 2002; Xoplaki et al., 2004) from October to March is considered. The homogeneity of the station precipitation time series have been assessed with GAHMDI (Toreti et al., 2010) and by Caussinus and Mestre (2004). Time series affected by more than two break points (i.e., change points due to non-climatic factors) are discarded. The extreme precipitation of the stations is analyzed with a procedure based on the generalized Pareto distribution in combination with other methods (Toreti et al., 2012).

The 5- and 50-year return levels are calculated and are shown in Figure I.10. The return levels (i.e., the level that is expected to be exceeded on average once every 5 and 50 years) help in understanding and quantifying the behavior of the most severe events. The 5-year return level map associated with the observations (Figure I.10A) highlights areas with very high values (e.g., the northern coast of Portugal, the Gulf of Lions, the Gulf of Genoa, Croatia, Rhodes, and the eastern Black Sea area) greater than 100 mm. Two stations in the western Mediterranean have a 5-year return level above 140 mm, while lower values are found with increasing distance from the coast. As for the 50-year return level map (Figure I.10B), the highest values are found at the western Iberian Peninsula, the Gulf of Lions, the western coast of the Balkan Peninsula, western Turkey, and the Black Sea area. An Italian station (Genoa) has the highest value, 264 mm.

For the most complete time series (fewer than 6 years missing), the series of exceedances are used to calculate the number of occurrences for each extended

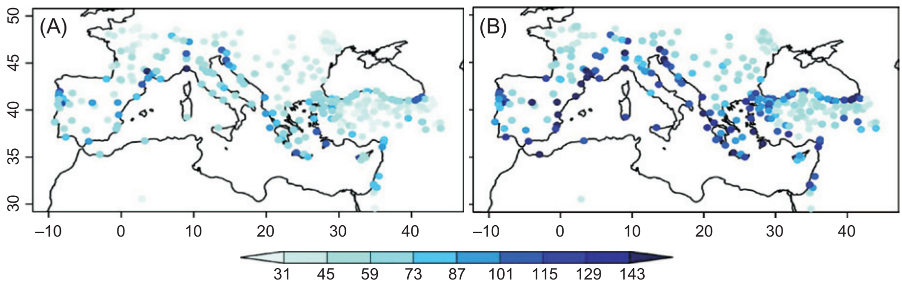

Figure I.10 (A) Five-year and (B) 50-year return levels of extended winter (October–March) precipitation (mm) estimated with daily precipitation time series from 1950 to 2006.

winter. Most of the series do not show significant changes; however, Greek series highlight a significant decreasing tendency in the occurrence of precipitation extremes. This indicates that the probability of observing an event above the threshold has decreased over the past 57 years. Those tendencies might be related to the decrease of the most intense Mediterranean cyclones (Trigo et al., 2000a; Bartholy et al., 2009).

I.9 Water Balance and Mediterranean Sea Circulation

In recent decades, great advances in observing technologies and systems have provided the scientific community with a rapidly increasing array of *in situ*, satellite, and marine data sets. Here is a brief summary of *in situ* data sets, climatologies, reanalyses, and remote sensing data that have provided the information for Chapter 4.

Oceanographic data profiles have been collected by different instruments during many oceanographic cruises and projects: CTDs (conductivity temperature depth recorders), XBTs (expandable bathy thermographs), and ADCPs (acoustic Doppler current profilers). A tentative list of contributing projects/cruises, not aiming at being complete, includes POEM and LIWEX, MATER, PRIMO, EUROMODEL, MEDGOOS, and, for new data collected since 2005, MEDOCC, CYCOFOS and CYCLOPS, CYBO, HaiSec, EYE of the Levantine, Alboran Glider Mission, METEOR, Medsudmed, APLABES, TUNIBAL, and the Bosphorus Tube Crossing Project. Further information is provided by mooring data (Eulerian measurements of currents, thermohaline and optical properties in fixed locations). Many of them are part of the Hydrochanges program by CIESM (the Mediterranean Science Commission) and are located all around the Mediterranean Sea at different depths.

The most important climatology available for the Mediterranean is the MEDAR/MEDATLAS II climatology (MEDAR Group, 2002; Rixen et al., 2005). Following the MEDAR joint effort to rescue, archive, and control the quality of Mediterranean and Black Sea data, 29,1209 temperature and 124,264 salinity profiles have been quality-checked and interpolated horizontally at 1° resolution and vertically at 25 standard vertical levels to provide gridded climatological fields. In several studies, the global climatology by Levitus et al. (2009) has also been used, particularly for the assessment of the warming of AW flowing into the Mediterranean Sea. Estimates of air–sea heat and freshwater fluxes and their components, wind stress, atmosphere and ocean variables, river discharges, and sea-surface temperature are provided by a number of reanalysis products (e.g., ERA40, NCEP/NCAR, ECMWF, ERA-Interim).

Remote sensed data are provided by several satellite missions: *Jason-1*, *Envisat* or *ERS-2, Topex/Poseidon*, and *Geosat Follow-On* (GFO) for altimetry data, *NOAA/AVHRR* and *MODIS* for thermal infrared images and sea-surface temperature, and *SeaWifs* and *MODIS* for ocean color.

I.9.1 Water Balance

The Mediterranean Sea is a concentration basin, i.e., it is characterized by a negative water budget. The excess of evaporation (E) over freshwater input is balanced by a two-layer exchange (G) at the Strait of Gibraltar, with a relatively warm and fresh upper-water inflow from the Atlantic and a relatively cool and saltier deep-water outflow to the Atlantic. The light and fresh AW is transformed into denser MW within the basin, through interactions with the atmosphere. Overall, the freshwater input in the Mediterranean Sea is given by the river runoff (R), precipitation (P) over the sea surface, and the inflow into the Aegean of Black Sea Water (B). The mass balance (M) is thus given by the relation $\mathrm{d}M/\mathrm{d}t = G + B + R - (E - P)$ The river runoff is far from being a negligible term for the Mediterranean Sea. Most estimates vary approximately 400–450 km^3/yr, equivalent to 160–180 mm/yr (see Section I.11).

Over the sea, large evaporation is experienced, especially in winter, because of the influence of northern dry and cold winds. Few direct observations of air–sea latent heat exchange are available, and Mariotti et al. (2002b) estimated the evaporation term in the range of 934–1176 mm/yr. With regard to precipitation, the annual mean over the sea ranges between 331 and 477 mm/yr (Mariotti et al., 2002a,b), but it has to be taken into account that direct measurements of precipitation over the sea are rare and that indirect estimations from coastal stations can be only approximate.

Combining the excess of evaporation and the river input, an estimated average Mediterranean freshwater deficit of about 480 mm/yr is obtained with a large uncertainty (~200 mm/yr), which in a steady state should be balanced by the freshwater inflow from the Black Sea and the Atlantic Ocean.

The Black Sea–Aegean Sea exchanges are as complex as the exchanges through the Strait of Gibraltar, with fresher water flowing from the Black Sea to the Mediterranean Sea at the surface and salty water flowing in the opposite direction below it. The net freshwater inflow into the Aegean is often simulated as a river flowing into the Mediterranean Sea, ranging between 75 (Lacombe and Tchernia, 1972) and 120 mm/yr (Kourafalou and Barbopoulos, 2003). This flux has an important interannual variability and long-term trends. Moreover, the decrease observed over the past few decades, mainly due to the building of dams along the Black Sea rivers and irrigation, might have had a role in the EMT (see Roether et al., 2007 for a review).

A critical point is that the flow rate at the Strait of Gibraltar displays a pronounced seasonal variability (García-Lafuente et al., 2007), which could in turn affect the long-term evolution of the flow rate by modulating the dense-water formation rate within the sea. Oceanographically based estimates of the water flux from the Atlantic Ocean at the Strait of Gibraltar are affected by strong uncertainties, and their temporal variability is largely unknown. The Strait of Gibraltar net volume transport gives an independent estimate of the mean value of the Mediterranean Sea freshwater budget, but up to now, these estimates (~640 mm/yr, averaged on values given by previous studies; see Mariotti et al., 2002b) do not agree with the *E–P–R* estimates (480 mm/yr). The agreement is even less if we include the Black Sea term (75–120 mm/yr).

I.9.2 Mediterranean Sea Circulation and Water Masses

The net freshwater loss through the surface in the Mediterranean Sea generates an inflow of AW in the surface layer, which spreads eastward (Bryden and Stommel, 1984). The westward return flow as well as the outflow at Gibraltar of denser MW takes place in deeper layers. The basinwide circulation pattern is prevalently cyclonic, as, especially in the western Mediterranean, the AW flows along the African coast and the return flow takes place prevalently along the northern shore (Millot, 1999). This general horizontal circulation pattern is perturbed by a number of subbasin-scale and mesoscale features (gyres and eddies) as well as by the dense-water formation processes that drive the intermediate and deep circulation cells. The eastern Mediterranean circulation gyres (Amitai et al., 2010) are semipermanent, to a large extent wind-generated, and positioned over some bottom features. On the other hand, the western Mediterranean is characterized by the formation of mesoscale eddies along the north African flow; their growth and propagation are toward the interior of the basin (Millot and Taupier-Letage, 2005b). The only semipermanent wind-driven feature is a dipole situated downwind of the Strait of Bonifacio in the Tyrrhenian Sea (Rinaldi et al., 2010). The two anticyclonic Alboran Gyres are also semipermanent features, but are probably due to thermohaline forcing (Viúdez et al., 1996a,b).

The thermohaline circulation patterns may be qualitatively traced following the temperature and salinity footprint of water masses, which tend to "conserve" those properties acquired in their formation regions. In general, a water mass is defined as a water volume with a common formation history, taking its origin in a well-defined region, where it acquires its characteristic properties. Outside its formation region, the water mass shares the space with other water masses, with which they mix (Tomczak, 1999). The water masses of the Mediterranean are characteristically different from those of the adjacent north Atlantic, due to the freshwater deficit and intense air–sea interactions. The climatological horizontal distributions of sea-surface temperature and salinity (see Figure I.11) show a clear west–east gradient of both parameters. A north–south gradient in temperature is also well evident in the temperature distribution. For salinity, the regions with lower values are those directly influenced by freshwater inputs (from the Atlantic Ocean, rivers, and the Black Sea),

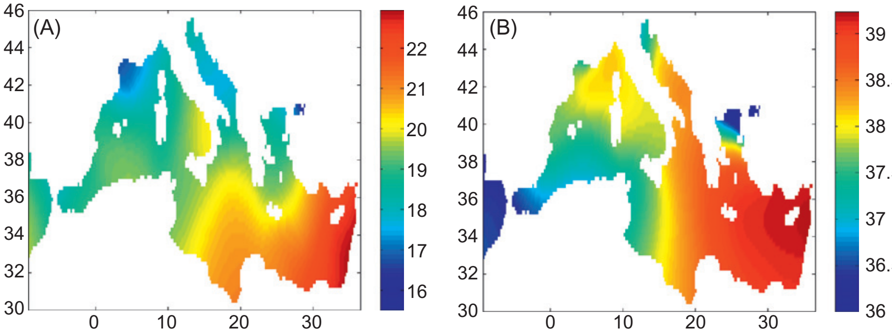

Figure I.11 (A) Climatological sea-surface temperature distribution. (B) Climatological sea-surface salinity distribution.
Source: MEDAR/MEDATLAS II database.

while the highest values in the easternmost part of the basin are due to the intense evaporation occurring over this region.

The general vertical structure of the whole basin is characterized by the presence of different water masses, which are clearly distinguishable in the different layers. In the Mediterranean, three main water masses may be identified:

1. Atlantic Water (AW), entering the Mediterranean at the Gibraltar Strait, which circulates through the whole basin increasing its temperature and salinity from west to east; it occupies a surface layer of approximately 100–200 m, with salinities in the range between 36.6 psu in the Alboran subbasin, 38.6 psu in the Ionian subbasin, and 38.9 psu in the Levantine subbasin; its temperature is mainly influenced by seasonal fluctuations.
2. Levantine Intermediate Water (LIW) is formed in the northeastern Levantine subbasin in the eastern Mediterranean and occupies the whole basin at intermediate depths (300–800 m); it is characterized by a relative maximum in temperature (15–16°C in the Levantine subbasin, 14–15°C in the Ionian subbasin, >13°C in the Alboran subbasin) and an absolute maximum in salinity (39–39.2 psu in the Levantine subbasin, >38.8 psu in the Ionian subbasin, >38.5 psu in the Alboran subbasin), both properties decreasing from east to west.
3. Deep Water (DW), which occupies the deep layer, is relatively colder and less salty than the intermediate water, originates during winter convection in the western Mediterranean (western Mediterranean deep water (WMDW), 12.7–12.9°C and >38.4 psu) and in the eastern Mediterranean (eastern Mediterranean deep water (EMDW), presently at 13.5°C and 38.7 psu). The EMDW formation shifted in the late 1980s/early 1990s from the Adriatic to the Aegean Sea characterizing the EMT.

The Mediterranean Sea circulation has obvious and strong implications with primary production, with features that are important for local fisheries (McCall, 2008) and whose variability can have physical, chemical, and biological effects. The Mediterranean Sea is globally considered as oligotrophic, or a low productive system. The inflow of nutrient-poor oxygenated Atlantic surface water into the Mediterranean, through the Strait of Gibraltar, associated with the basinwide

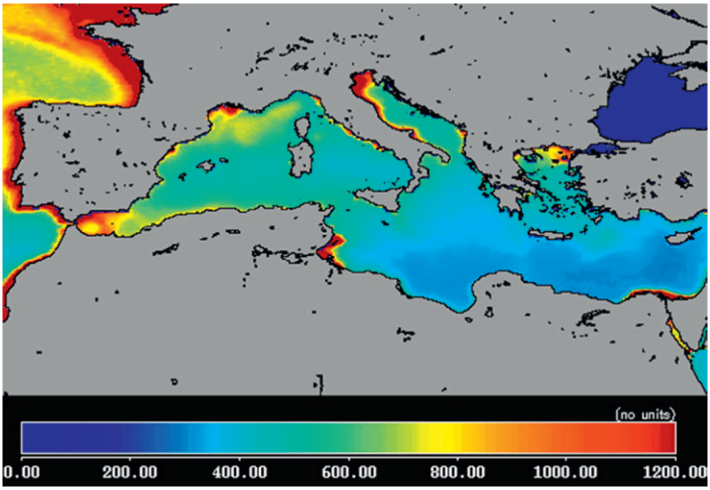

Figure I.12 Ten-year annual mean NPP for the Mediterranean region. The map was generated from *SeaWiFS* chlorophyll distributions according to the Vertically Generalized Production Model (VGPM) (Behrenfeld and Falkowski, 1997). The map uses a cylindrical projection, and one pixel = 1/12°.
Source: The map was provided by http://www.science.oregonstate.edu/ocean.productivity

cyclonic circulation of nutrient-depleted water (Dugdale and Wilkerson, 1988), hot and dry climate, and low land runoff, contribute to the low productivity and to a west-to-east increase in oligotrophy (Caddy, 1993). This is clearly visible in Figure I.12, with high levels of net primary production (NPP) in the Alboran subbasin along the Spanish coast and low levels in the southeastern Mediterranean. However, there are other areas of relatively high NPP, such as those due to nutrient discharge from land runoff from the Rhône and the Po (Béthoux, 1981). This factor is further reinforced in the Gulf of Lions by the occurrence of upwelling during strong northwestern winds (Mistral) (Minas, 1968; Estrada, 1999) and winter deep convection (San Feliu and Muñoz, 1971; Estrada, 1999). Also in the Adriatic, the Ligurian and Tyrrhenian subbasin gyres and upwelling contribute to high phytoplankton productivity. Local NPP maxima also occur in the Catalan coast of Spain, where wind-driven upwelling may occur in winter (Margalef and Castellví, 1967; Fiuza, 1983; Estrada 1999).

I.10 Present Mediterranean Sea Level

Sea level is an important oceanic parameter, possibly the most important in relation to impacts (Nicholls et al., 2007), particularly when taking into account that today 10% of the world's population lives within 10 m of mean sea level (Mcgranahan et al., 2007) and that this percentage goes up to 34% in the Mediterranean region

(Lionello et al., 2006a). Changes of sea level gradually increase the pressure on the coastal environment, eventually forcing the coastlines to retreat or to develop new coastal protection. Knowledge of the extreme sea-level values and of their variation is very important as well, because extreme events are the main cause of damage and source of risks.

At long timescales (interannual to interdecadal), the major contributors to sea-level variability are the mass addition or removal from the oceans by glaciers, ice caps, and ice sheets (the mass component); changes in the volume of the water body due to changes in its density (the steric component); and, at the regional scale, the contribution of atmospheric pressure and wind (the atmospheric component). Relative sea level is also affected by the postglacial rebound and isostatic adjustment, tectonic motions, and local subsidence (e.g., due to loss of groundwater). Separating the contribution of each of these factors is not a trivial task. Nevertheless, it is essential because it permits the assessment of the significance of each forcing factor and, consequently, an assessment of future changes under climate-change scenarios.

On the assumption that changes in the Mediterranean basin are represented by the available observations (see Figure 4.1a), sea-level variability over the past century can be separated into three periods. Before the 1960s, Mediterranean Sea level had trends equivalent to those of open ocean stations (1–2 mm/yr). Between 1960 and the beginning of the 1990s, sea level was either not changing or even decreasing. The third period, between 1993 and the early 2000s, has been characterized by a fast sea-level rise (several mm/yr). This behavior is reflected in individual tide-gauge records as well as in the Mediterranean mean sea-level reconstruction shown in Figure I.13. Overall, it is widely accepted that during the second half of the twentieth century, the Mediterranean mean sea level has been rising at a rate of about 0.6 ± 0.1 mm/yr, which is less than a half of the rate of global mean sea-level rise (e.g., 1.6 mm/yr for

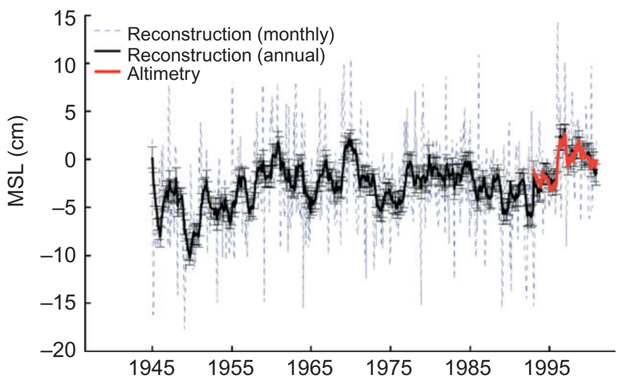

Figure I.13 Mediterranean mean sea level derived from the sea-level reconstruction carried out by Calafat and Gomis (2009); both monthly and annual values are represented, the latter with the corresponding error bars. The red line corresponds to annual values of Mediterranean mean satellite altimetry.

the period 1961–2000, for which the trend of Mediterranean mean sea level was even lower: 0.2 ± 0.1 mm/yr).

The reasons why Mediterranean mean sea level has been rising at a lower rate than global mean sea level are thought to be the increase of atmospheric pressure over the region and a negative steric effect. The individual contributions to the sea-level budget for the period 1945–2000 have been estimated at −0.4 ± 0.1 mm/yr for the atmospheric contribution, –0.3 ± 0.1 mm/yr for the steric contribution, and +1.2 ± 0.1 mm/yr for the mass addition. The negative steric component results from a salinity increase superimposed on a slight temperature decrease when averaged over the whole basin, as inferred from existing hydrographic databases. It is worth noting, however, that while temperature changes result in effective volume expansions/contractions, salinity changes also involve changes in the mass of the basin, so that the steric and the mass component must be considered together when doing the physical interpretation of salinity changes (see Chapter 4 for the details). It must also be stated that the trends reported for the sea-level components have an associated uncertainty of at least 0.1 mm/yr (probably larger for the steric component) when estimated on a 50-year long interval, which justifies the small discrepancy between the best estimate of sea-level rise and the algebraic sum of the individual contributions.

Less has been published on sea-level extremes, whose observation is partly handicapped by the long repeating cycle of satellite altimeters (10 days in the best case) and the sampling interval of tide gauges (often 1 h, which does not allow the detection of high-frequency events such as the so-called meteotsunamis). Reliable statistics are limited to sea-level extremes associated with storm surges, which are usually modeled fitting the tail of sea-level histograms to a theoretical known parametrical function. The studies dealing with sea-level extremes have identified regional rather than generalized changes in storminess, and most of the interannual and decadal variability observed at the basin scale seems to be caused by mean sea-level changes.

I.11 River Runoff

Geographically, the Mediterranean catchment is extremely large and heterogeneous, covering an area of approximately 5 million km^2. It extends from the equator, where the springs of the White Nile River are located, to the source of the Rhone River at approximately 48°N. In longitude, it spans about 40°, from the middle of the Iberian peninsula, at 4°W, toward southern Turkey and the Middle East coasts facing the Mediterranean Sea (35°E)

Because of the presence of many mountains all around the basin, most of the Mediterranean catchment is morphologically quite complex and consists of only few great valleys, corresponding to the main rivers flowing into the Mediterranean (such as the Nile, the Rhone, and the Ebro) and a couple of large alluvial plains (the Po plain and the Nile Delta). For the remaining, it is characterized by many rivers that flow through narrow valleys and collect water from the surrounding mountains. Regions of northern Africa extending from the Atlas mountains to the Nile Delta

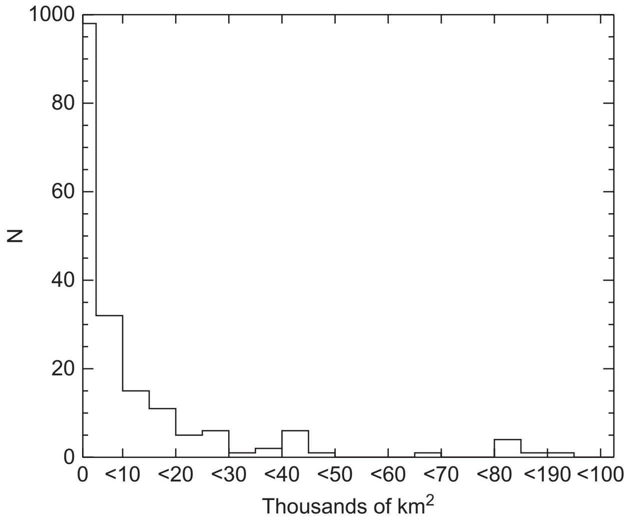

Figure I.14 Distribution of catchment areas within the Mediterranean basin (Nile not included).

are instead characterized by moderate elevation and by a few creeks that become dry during the summer season. Figure I.14 shows the distribution according to their extension of 186 different catchments that have been identified all around the Mediterranean basin, by means of the TRIP (Total Runoff Integrated Pathways) database. Only a few major catchments cover an area greater than 80,000 km^2, while most of them are concentrated between medium and small extensions. The Nile basin, which covers an area of approximately 3,400,000 km^2, is not included in the plot.

The annual mean freshwater supplied to the Mediterranean Sea by the rivers discharging into it has been estimated $8.0 \times 10^3\,m^3/s$, according to a data set of observed monthly discharge time series of 68 rivers (Struglia et al., 2004). Such a value is necessarily an underestimate, as observations are not available for many rivers, with poor data coverage mainly for the southern and eastern regions. Other estimates available in the literature, including inventories of major rivers, mapping of average runoff depths, and modeling vary approximately 400–450 km^3/yr, i.e., 12.7–$14.3 \times 10^3\,m^3/s$ (Ludwig et al., 2009).

The four major Mediterranean catchments (Ebro, Rhone, Po, and Nile) contribute to this value, with an annual mean of $4.9 \times 10^3\,m^3/s$ (i.e., slightly more than 60% of the measured total). These considerable local injections of freshwater into the Mediterranean Sea are extremely important for the thermohaline circulation of the whole Mediterranean Sea. Freshwater anomalies, in conjunction with winter cooling, can affect the processes of dense-water formation in the Gulf of Lions, the North Adriatic, and the Levantine Sea.

Figure I.15 shows the mean annual seasonal cycle of total Mediterranean river discharge, calculated from historical time series of the TRIP observational data set

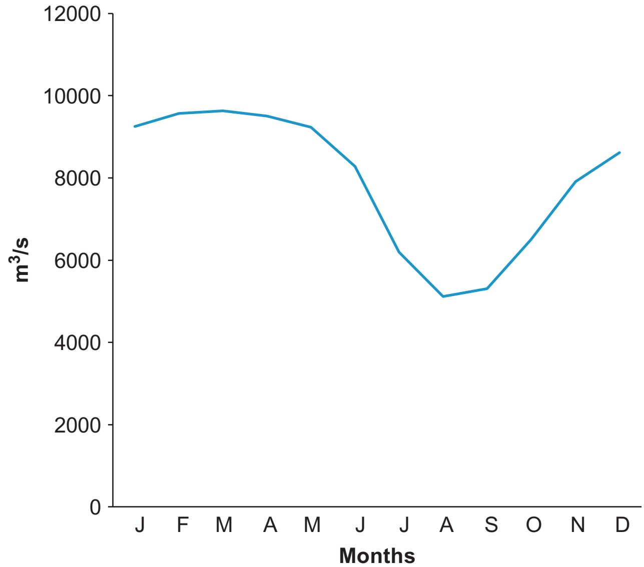

Figure I.15 Mean annual seasonal cycle of total Mediterranean river discharge, calculated from historical time series of the observational data set.

(Oki and Sud, 1998). The period covered by observations spans mainly the years 1960–1990. The mean seasonal cycle is characterized by high values of discharge, exceeding the annual mean value, from autumn to late spring, with a deep minimum during the summer. This seasonality depends on the characteristics of precipitation in the Mediterranean area, as well as on the geographical characteristics of the catchment. The Alps, where most of winter precipitation is in form of snow, ensure an important contribution to freshwater until late spring. The other mountains, such as the Atlas in northeastern Africa, the Dinaric Alps in the Balkans, and the Taurus in Turkey, are effective in capturing moisture by means of orographic effects from eastward-propagating midlatitude cyclones generated in the north Atlantic Ocean and in the eastern Mediterranean Sea, during fall and winter.

I.12 Cyclone and Main Synoptic Patterns

The Mediterranean Sea is characterized by intense synoptic scale activity, and the northern hemisphere storm track presents a separate branch crossing the Mediterranean region, with areas of cyclogenesis in the western Mediterranean and of prevalent cyclolysis in the central and eastern Mediterranean (Lionello et al., 2006b and Chapter 3). Though shallower, with a smaller extension and shorter lifetime than their counterparts in the north Atlantic storm track, the Mediterranean cyclones cause extreme precipitation, storm surges, and wind storms (Lionello et al., 2006b). The complex morphology of the Mediterranean region has an important role

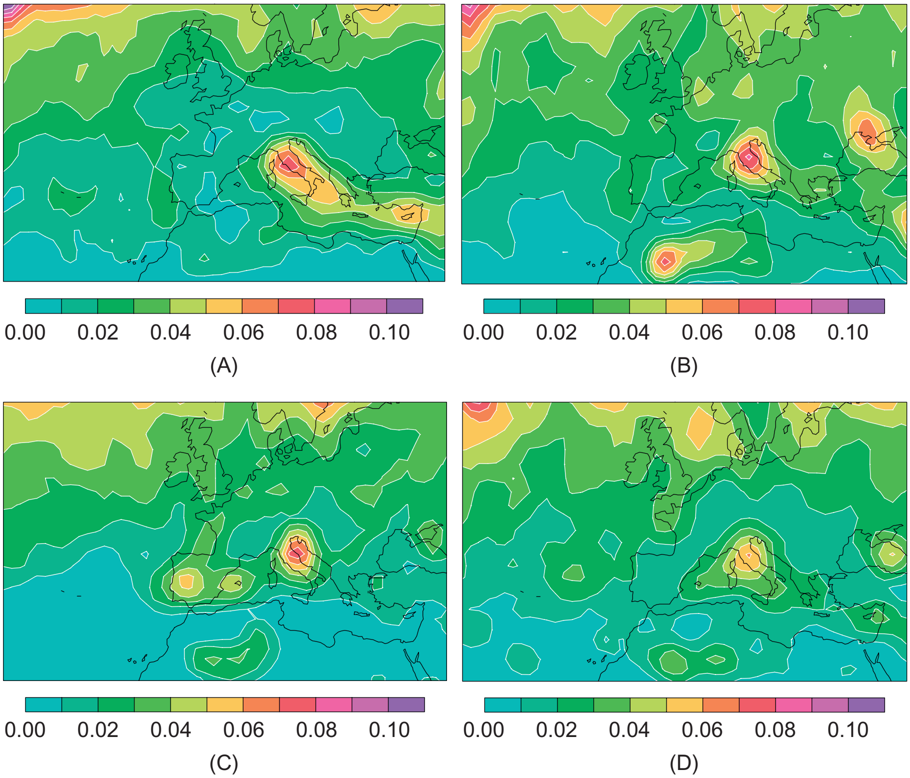

Figure I.16 Seasonal average density track (seasonal frequency/degree^2) according to ERA-Interim 1989–2009 in winter (A), spring (B), summer (C), and fall (D). Only cyclones with a minimum duration of 1 day and 5 hPa depth with respect to the background are included.

in the generation and evolution of Mediterranean cyclones. The most well-known example is the orographic cyclogenesis area south of the Alps in the Gulf of Genoa (Buzzi and Tibaldi, 1978), but other features are also important, such as the strong temperature contrast between the Mediterranean Sea and the north Africa areas for the generation of Sharav cyclones south of the Atlas mountains (Alpert and Ziv, 1989). Furthermore, local features are crucial because they enhance the effects of cyclones by constraining the circulation in the lower troposphere; an example is the channeling of the wind along the Adriatic producing a storm surge in Venice (Trigo and Davies, 2002; Lionello, 2005) and the advection of moisture with consequent intense precipitation on the coastal ridges (Buzzi et al., 2005; Homar et al., 2007).

The phenomenology of Mediterranean cyclones is rich and complex. Figure I.16 shows the density of storm tracks in the Mediterranean based on the tracking algorithm by Lionello et al. 2002. Note that, in general, tracking results, such as the relative importance of the various features in Figure I.16 as well as their precise location, depend on the details of the cyclone identification and tracking algorithms used (see Figure 3.4). The comparison among the existing methods is an issue of current research, but it is evident that the choice of the most suitable method will depend on the scientific problems to be addressed in a specific study.

Figure I.16 shows a strong seasonality, with the relative importance of the different parts of the tracks changing during the year. The track density is most intense in winter, when cyclone tracks are frequent in large parts of the Mediterranean in a band from northwest until to Middle East coast. It should be noted that the maxima in Figure I.16 are mainly produced by shorter cyclone tracks rather than by lows traveling through the whole basin. north African cyclones are the dominant feature in spring (Figure I.16B). Stationary low-pressure centers are frequent in summer over Iberia, northern Italy, and the western Mediterranean. Again, note that the relative importance of these features depends on the specifications used in the identification and tracking algorithms, as becomes evident when comparing Figures I.16C with Figure 3.5A. The different mechanisms responsible for this variability are space and time, and their links to large-scale circulation patterns are reviewed in Chapter 3.

I.13 Mediterranean Winds

A number of winds with a seasonal characterization occur in the Mediterranean region. Figure I.17 shows the seasonal mean wind speed and direction from the daily *QuickSCAT* data (Chronis et al., 2010). During winter (DJF) (see Figure I.17A), wind speed exhibits the highest mean values as compared with any other season. Throughout the year, the Gulf of Lions sustains wind magnitudes higher than 7 m/s (see Figure I.17A–D), largest during winter (8–11 m/s), extending its influence to the northeast and over the Ligurian subbasin. The Aegean shows one of the most distinctive features, with the wind lobes to the east and west of the island of Crete corresponding to the exit points of the northerly flow. These features are dominant during summer (Etesian winds) (Maheras, 1980; see Figure I.17C) but present during all seasons. One prominent feature is the wind direction reversal over the Balearic subbasin between winter and summer (from northwesterly winds) (see Figure I.17A) to northeasterly winds (see Figure I.17C; Dorman et al., 1995; Losada, 1999). Over the Adriatic, an easterly/northeasterly flow is present during winter, spring, and fall, while during summer, the dominant regime corresponds to the generalized northerly flow that occurs over the eastern Mediterranean (see Figure I.17C).

Maps showing the names of main Mediterranean winds can be found in Lionello et al. (2006b) and in Chapter 3. Going from west to east, one may identify the easterly Levanter and its westerly counterpart Poniente, affecting the Strait of Gibraltar and the Alboran. Over the Gulf of Lions and the Ligurian subbasin, the cold dry Mistral blows from the north northwest, repeatedly reaching the southern Mediterranean shore and as far as the Ionian subbasin. The Mistral is a strong jet that dominates mainly in winter, while during summer it is highly reduced. The influence of the Mistral into the Tyrrhenian is regulated by an upper-level depression that develops over the Ligurian subbasin, ranking this area as one of the most active cyclogenic centers in Europe (Flocas, 1988; Trigo et al., 2000b). During winter, the northeasterly Bora dominates over the Adriatic and Aegean (Bergamasco and Gacic, 1996; Poulos et al., 1997; Paklar

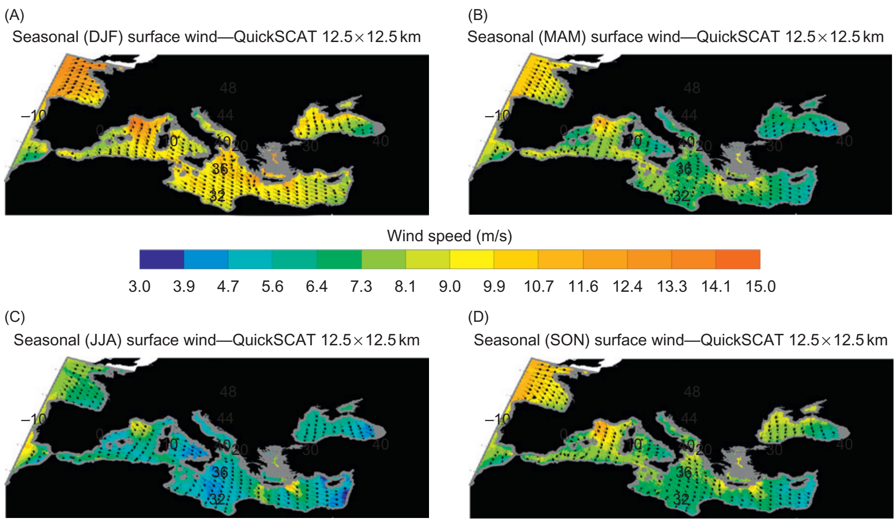

Figure I.17 Seasonal mean (2000–2008) wind magnitude/direction from QuickSCAT for (A) Winter (DJF), (B) spring (MAM), (C) summer (JJA), and (D) fall (SON). The gray color relates to grid points that did not pass the quality filtering (i.e., coastal areas). *Source*: Chronis et al. (2010). Reproduced by permission of John Wiley and Sons.

et al., 2001), while during summer–early fall the pressure gradients between eastern Europe and Anatolia give rise to the Etesian winds, which further intensify over the Aegean (Maheras, 1980; Lascaratos, 1992). The southwesterly (Sirocco) winds from the northern African coast are observed during fall and spring (Hadjimichael et al., 2002). Both the Mistral and the Etesian wind regimes play an important role in the dense-water formation processes that occur in the western and eastern Mediterranean, respectively. In general, over the Mediterranean Sea, wind and wind stress curl are as important as heat and water fluxes for explaining the features of the Mediterranean Sea circulation (Malanotte-Rizzoli and Bergamasco, 1989; Pinardi and Navarra, 1993; Roussenov et al., 1995; Zavatarelli and Mellor, 1995; Herbaut et al., 1996; Borzelli et al., 2009).

Romanou et al. (2010) showed that the Mediterranean wind pattern is characterized by localized extremes, such as the large values over the Gulf of Lions, the Cretan Passage, and the Kassos Straits. High wind variability occurs over the western and central basins (the Balearic, Tyrrhenian, and Ionian subbasins), as well as south of Crete, being very low over the eastern Levantine subbasin (Romanou et al., 2010).

I.14 Wind-Generated Waves

Ocean waves are an important component of the Mediterranean environment. They represent a key factor influencing offshore activities, ship traffic, and most importantly, determining the evolution of the long Mediterranean coastline (46,000 km) and the size and type of coastal protections. Waves are the consequence of strong winds (such as Bora, Mistral–Tramontane, Etesian, Sirocco, and Libeccio) blowing over the basin (Lionello et al., 2006b) and are associated with the passage of cyclones in the region. The Mediterranean Sea is characterized by intense synoptic-scale activity, and the northern hemisphere storm track presents a separate branch crossing the Mediterranean region, with areas of cyclogenesis in the western Mediterranean and of prevalent cyclolysis in the central and eastern Mediterranean (Lionello et al., 2006b). Therefore, waves provide an indirect estimate of storm-track intensity and location and wind daily variability, which is the timescale typical of wind-wave generation.

In general, wave analyses are based on significant wave height (SWH), which is a statistical parameter that is proportional to the total variance of the sea surface and a good representation of the visual estimate of wave height at sea. Since instrumental wave records are too sparse and satellite time series too short for the identification of climate trends, most results are based on model simulations forced by simulated wind fields. Therefore, the availability of correct high-resolution winds is a basic requirement for wave modeling. In general, underestimates of the wind speed and missing sharp features in the wind fields are sources of similar shortcomings in the computed SWH fields (Cavaleri and Bertotti, 2004). Unfortunately, instrumental wave records are too sparse and satellite time series too short for the identification of climate trends and computation of robust climate fields, while numerical simulations have been shown to provide a reliable representation of the real space and time SWH variability (Lionello and Sanna, 2005).

In general, high SWH values are caused by strong winds with a long fetch. Simulations (Figure I.18) show the highest values in the western Mediterranean under

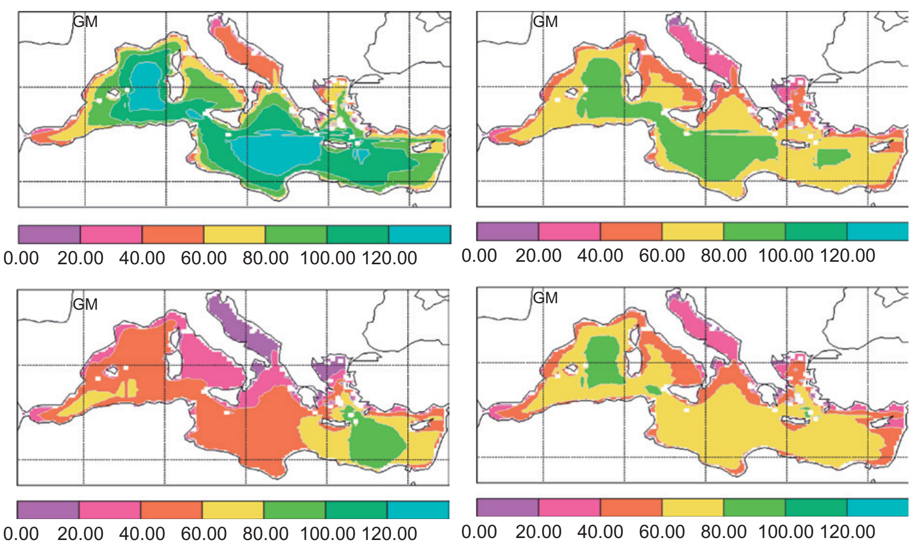

Figure I.18 Seasonal 50th percentile SWH distribution (winter: DJF, spring: MAM, summer: JJA, autumn: SON; units are centimeters) based on a hindcast study for the period 1958–2001.

the effect of the Mistral wind. Other maxima are located in the southern Ionian Sea and the Levantine basin. The northern Aegean and the whole Adriatic are the basins where mean SWH are lowest. In summer, the action of the Etesian winds produces a well-defined peak in the Levantine basin.

I.15 Aerosol Climatology over the Basin

Aerosol particles are now recognized as one of the environmental variables that can play a significant role on the regional climate through their direct radiative impact on solar radiation and indirect radiative impact due to their interaction with clouds. For instance, simulations of the regional climate in the Indian Ocean have shown that aerosol forcing during the dry season has implications for the precipitation pattern during the following wet monsoon season over India (Ramanathan et al., 2001). However, the quantification of radiative effects of natural and anthropogenic aerosols in the Mediterranean region is at an early stage and subsequent effects on the regional climate and possible feedbacks still need to be assessed. Here, we describe the distribution of the tropospheric aerosol over the Mediterranean based on recent satellite data and report scarce available data on their radiative forcing and impacts on precipitation. We focus on the distribution of aerosols over the sea because the Mediterranean marine troposphere is strongly perturbed by particles of continental origins, whereas marine areas usually experience low aerosol concentrations. In addition, it is over the sea surface that dimming by aerosols is likely to have the most important effect by decreasing surface evaporation, since the Mediterranean Sea is the main source of moisture for precipitation in many land areas around the basin (Gimeno et al., 2010).

I.15.1 Variability

Aerosol transport models indicate that the average aerosol load over the Mediterranean basin is dominated by particles from the surrounding continental sources, especially desert dust, and is larger than over other regional European seas, and even larger than over most of the European continental regions (Textor et al., 2006).

Aerosol monitoring can be made in cloud-free conditions in terms of aerosol optical depth (AOD) at the basin scale using satellite measurements of the backscattered solar radiation, with validation by ground-based sun photometer measurements (Holben et al., 1998; Bréon et al., 2011). AOD is a measure of the attenuation of the incident solar radiation through the atmosphere. Satellite observations have shown that the Mediterranean tropospheric AOD is dominated by desert dust from Africa due to the occurrence of occasional dust outbreaks (Moulin et al., 1998; Barnaba and Gobbi, 2004; Antoine and Nobileau, 2006; Santese et al., 2007; Gkikas et al., 2009). Dust is associated with the highest peaks in AOD (>1), but relatively high turbidity events can also be due to anthropogenic pollution and biomass burning (Pace et al., 2005; Papadimas et al., 2009).

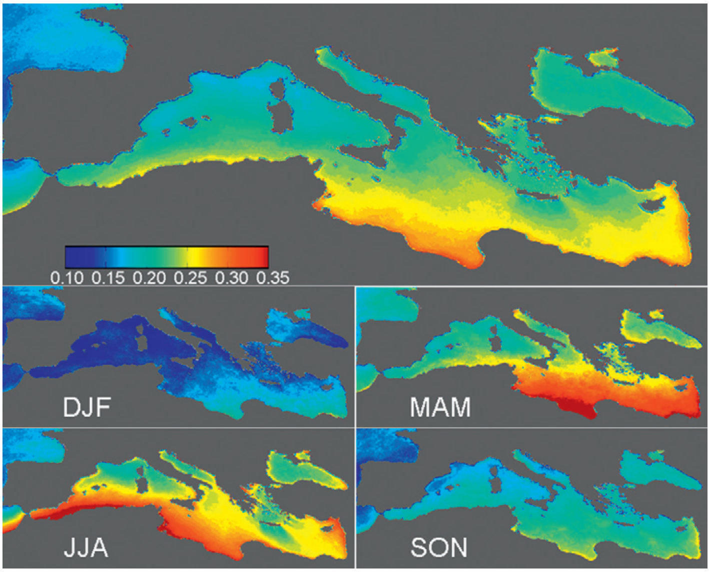

Figure I.19 Map of the mean aerosol optical depth at 550 nm (AOD) for the 5-year period from June 2005 to May 2010 and corresponding seasonal averages as derived from MSG/SEVIRI following the method of Thieuleux et al. (2005). The overall average is 0.26 ± 0.04 (Black Sea and Atlantic excluded). In this retrieval, a limitation of the cloud coverage of a given pixel is obtained by taking advantage of the MSG 15 min time resolution: daily AOD is averaged from the inversion of up to 33 time slots between 8:00 and 16:00 UT. For the 168,092 Mediterranean pixels, this results in an average number of 1112 ± 264 days with clear-sky retrievals over the considered period of 1826 days. The pixel size is 3 × 3 km at nadir and varies from about 11 to 22 km^2 over the Mediterranean. It should be noted that the discontinuity in AOD observed in the first two marine coastal pixels (lines of maximum and minimum AOD along the coast) is an artifact resulting from the EUMETSAT resampling process of raw MSG/SEVIRI pixels into the level 1.5 reference frame, which is enhanced by the aerosol processing in the presence of a sharp contrast in reflectance, such as the coastline.

Figure I.19 shows a recent 5-year climatology of the AOD over the sea derived from the Meteosat Second Generation, Spinning Enhanced Visible, and Infrared Imager (MSG/SEVIRI) satellite instrument. The geostationary MSG/SEVIRI instrument is chosen here among other satellites producing AODs because it offers by far the best coverage of the basin, with, on average, more than 60% of days covered at the pixel scale (Thieuleux et al., 2005 and Bréon et al., in press) for evaluation of the AOD retrieval from SEVIRI using AErosol RObotic NETwork (AERONET) data. The overall average in AOD is 0.26 ± 0.04. The north-to-south-increasing AOD illustrates the major role of desert dust. The maximum in AOD occurs in the central basin, which experiences the longest dust season. On average, the northward transport of African dust starts in early spring in the eastern basin and progressively extends westward to peak in the Alboran Sea in summer. A secondary maximum occurs in fall. The dust transport is mainly associated with thermal low-pressure systems forming over north Africa, and with north Atlantic lows passing over Spain (Moulin et al., 1998).

The mean aerosol distribution is also clearly related to the precipitation distribution, since the aerosol residence time and its long-range transport are limited by scavenging by precipitation (Bergametti et al., 1989; Moulin et al., 1998; Barnaba and Gobbi, 2004). This combination of factors explains a significant winter minimum in AOD over the basin. A noticeable exception to the correlation between seasonal AOD and rainfall is found in summer over the dry eastern basin, where the relatively low AOD is due to the dominant northerly Etesian winds that prevent dust export over the basin (Moulin et al., 1998).

Multiyear studies of AOD always show a strong interannual variability, and this is the case over the Mediterranean region (Moulin et al., 1998; Antoine and Nobileau, 2006; Papadimas et al., 2008, 2009; Gkikas et al., 2009). The latitude of transport of humidity from the north Atlantic to western Europe is related to the north Atlantic pressure dipole between the Icelandic low and the Azores high, and a significant correlation between dust summer or annual AOD and the preceding winter NAO index has been reported over different periods from early satellite-derived AOD products in 1983 up to now (Moulin et al., 1997; Antoine and Nobileau, 2006; Papadimas et al., 2008; Gkikas et al., 2009).

Part of the seasonal and regional variability in AOD over the Mediterranean basin is due to nondust fine (submicronic) continental aerosol. They show an average south-to-north and west-to-east increasing gradient and also a summer maximum (Barnaba and Gobbi, 2004). By contrast, sea salts contribute to a relatively constant seasonal and geographical background in AOD (Barnaba and Gobbi, 2004).

I.15.2 Radiative Impact

In the early 1990s, the radiative forcing effect of anthropogenic sulfate aerosols was found to counteract the anthropogenic greenhouse-gas forcing on a global average, but with a much higher temporal and geographical variability due to the short lifetime and subsequent heterogeneous distribution of aerosols (Charlson et al., 1992). Global simulations revealed that the sulfate aerosol forcing was clearly dominant at regional scales, and it was found to be especially high in the Mediterranean region (Le Treut et al., 1998). The so-called parasol effect of atmospheric aerosols results from increasing reflection back to space of incoming solar radiation, due to increased atmospheric scattering by particles (direct effect) and by clouds (indirect effects). The indirect forcing effects result from a reduction in cloud droplet size due to an increased number of condensation nuclei, a reduction well observed over continental areas and the Mediterranean as compared with remote oceanic areas (Bréon et al., 2002). The related increase in reflection of solar light is due to both an increase in cloud albedo (first indirect or Twomey (1974) effect) and cloud lifetime (second indirect or Albrecht (1989) effect). In addition, aerosols absorbing light cause both additional decrease in solar irradiance at the Earth surface (and thus in latent heat flux due to evaporation) and heating of turbid atmospheric layers (semidirect effect) that may exceed 1 K/day over remote marine areas for Saharan dust (Carlson and

Benjamin, 1980) or carbonaceous aerosols (Léon et al., 2002), and thus limit the marine stratocumulus cloud cover (Ackerman et al., 2000; Johnson et al., 2004).

Mediterranean aerosols are relatively absorbing because of the abundance of both desert dust and carbonaceous particles (Formenti et al., 2002; Markowicz et al., 2002; Meloni et al., 2006; Roger et al., 2006), with a single scattering albedo averaging between 0.90 and 0.95 (Bergamo et al., 2008). Their absorption in the atmospheric column modifies atmospheric stability and enhances solar radiation deficit at the surface. Tragou and Lascaratos (2003) show that aerosols might explain the long-term solar radiation that is 25 W/m^2 weaker than expected that is observed at the surface in the Mediterranean, especially in summer, and also its interannual variations. A few studies combining aerosol radiative measurements and computations estimated daily aerosol direct radiative surface forcing for nondust aerosols in clear-sky conditions between -18 and -47.5 W/m^2 near Marseilles (Roger et al., 2006), at Lampedusa Island (Meloni et al., 2003), and at Finokalia in Crete (Markowicz et al., 2002). A comparable number of -37 W/m^2 was obtained during a dust transport event over Lampedusa (Meloni et al., 2003). Besides these case studies in clear-sky conditions, Bergamo et al. (2008) estimated the whole-sky anthropogenic aerosol direct radiative forcing for the year 2003 at five AERONET sun photometer monitoring coastal stations in the Mediterranean basin. Results at the surface are about –3 W/m^2 at the southernmost stations of Lampedusa and Crete, and about -5 W/m^2 at the other stations in Sardinia, Lecce, and Venice, and about -2 to -2.5 and -3 W/m^2, respectively, at top of atmosphere (ToA). Comparable numbers for the 2001–2003 annual ToA direct radiative forcing by anthropogenic aerosols and somewhat larger numbers for the surface forcing were obtained over the Mediterranean from global computations using aerosol and cloud remote-sensing data by Chung et al. (2005). Indirect effects are likely to reinforce ToA and surface aerosol radiative forcing, and there is no doubt that the anthropogenic aerosol forcing is more important than the forcing by greenhouse gases in the Mediterranean at the yearly timescale. It is, thus, likely that the radiative budget of aerosols influences the regional climate at least during the dry, high-aerosol season.

I.15.3 Impact on Precipitation

A large-scale climate model simulation suggests a 15–30% decrease in precipitation over the Mediterranean basin due to aerosol-derived reduction of evaporation, with a delayed response between the maximum summer aerosol direct forcing and the following rainy season (Lelieveld et al., 2002). In addition to direct radiative effects, aerosol properties play a complex role in cloud formation and life cycle, and hence influence the distribution and amount of precipitation, depending on the type (warm/cold, continental/maritime) of cloud (Pruppacher and Klett, 1997). The increase in the number of cloud condensation nuclei (CCN) over the basin due to high loads of anthropogenic aerosols there (Bréon et al., 2002) most probably contributes to additional inhibition of precipitation as compared with a purely maritime atmosphere by producing more but smaller cloud droplets (Albrecht, 1989; Xue and Feingold, 2006).

Studies of the impact of aerosol on precipitation in the Mediterranean has been somewhat focused on the microphysical effects of desert dust particles. Dessens et al. (2007) have suggested that the most severe hailstorms in South-West France are generally associated with Saharan dust events, but whether the dominant cause is microphysics or dynamics is unclear. Mineral dust particles were recognized early on as being efficient ice nuclei (Isono et al., 1959), and it was suggested that reevaporation of ice crystals left dust particles with enhanced cloud-condensation properties (Mason and Maybank, 1958). Mineral dust particles were especially found to initiate freezing of supercooled cloud droplets at temperatures down to about −10°C (i.e., at much less cold temperatures than usual) from both laboratory (Mason and Maybank, 1958) and field (Rosenfeld et al., 2001; DeMott et al., 2003) observations, thus affecting cloud phase. Condensation of water prior to ice is not observed on the most abundant mineral-dust phases (Zimmermann et al., 2008), but Wiacek et al. (2010) indicate that air-mass trajectories affected by dust generally reach cirrus-forming regions after processing in mixed-phase clouds. Observations in the eastern Mediterranean confirm that cloud-droplet evaporation leaves mineral dust particles with coating by soluble sulfate (Levin et al., 1996) or sea salt (Levin et al., 2005). The mass of soluble salts increases with the number of condensation–evaporation cycles (Wurzler et al., 2000). Microphysical model studies indicate that this yields giant efficient CCN producing larger cloud drops and accelerating the development of precipitation (Wurzler et al., 2000; Yin et al. 2002). This has a relatively low impact on precipitation in marine types of clouds, however, since sea-salt particles already provide such large CCNs (Yin et al., 2002; Levin et al., 2005). In continental clouds, competing effects of dust between the production of large CCNs accelerating rain formation and large increase in the number of small CCNs may well result in a net decrease in total precipitation (Rosenfeld et al., 2001; Yin et al., 2002). However, some observational claims about the potential impact of pollution on orographic precipitation in Israel were shown not to be substantiated and perturbed by other urbanization effects (Alpert et al., 2008). These studies on dust microphysical effects show that assessing the regional impact of aerosols on Mediterranean precipitation is a very complex issue. Reducing uncertainties will require new dedicated process studies on atmospheric water–aerosol particle interactions and their parameterization in regional coupled climate models.

I.16 Future Climate

According to the last IPCC report (IPCC-WG1, 2007), this region is one where there is a great consistency in model results concerning the risk of drying during this century (G1 report, chapter 11, box 11.1, and figure 2). This critical condition is also shown by the climate-change indexes computed by Giorgi (2006).

Giorgi and Lionello (2008) reviewed climate-change projections over the Mediterranean region based on an ensemble of 17 GCM (Global Climate Model) simulations extracted from the MGME (Multi-Global Model Ensemble) stored at the Program for Climate Model Diagnosis and Intercomparison (PCMDI) (http://www-pcmdi.llnl.gov). A robust and large warming is projected, with a maximum in the summer season. Figure I.20 shows the ensemble temperature increase of the 2071–2100 period as compared with the 1961–2100 period for the A1B emission scenario. In summer (June–July–August (JJA)) values reach 3–4°C over the sea and grow further to 4–5°C in inland areas, with maxima higher than 5°C in the Sahara and Middle East. Projections agree also on a pronounced decrease in precipitation, especially in the warm season, except for the northern Mediterranean areas (e.g., the Alps) in winter. Figure I.20B shows the ensemble change of precipitation for the same periods and scenario as in Figure I.20A. The reduction in precipitation is smallest in winter, varying from no change in the northern Mediterranean to a 40% reduction in the south. In spring and fall, reduction of precipitation varies between 10% and 40%. The average value of the large summer reduction is in the range 25–30%, but some areas in the northeast and the south show a decrease that is larger than 50%. Further details and discussion of how this compares with RCM and statistical model results, as well as a discussion on the change in variability can be found in Chapter 8.

Regional sea-level projections for the twenty-first century are very preliminary. Though all models show an increase in both temperature and salinity over this century, the steric effect of these changes can give positive or negative sea-level trends depending on whether temperature or salinity dominates. There is also a lot of variability at the subregional scale, with different regions experiencing either a positive or a negative trend in the same simulation. These uncertainties need further investigation with a large ensemble of simulations and a better evaluation of each contribution to sea-level change. In fact, the trend of the mass component is uncertain as well. This is essentially linked to the evolution of sea level in the nearby Atlantic, which in turn depends on remote processes such as the melting of continental ice. It must be stressed that none of the RCM simulations used to infer future sea level accounts for ice melting. Understanding the role of the Strait of Gibraltar will be crucial to link sea level in the Mediterranean and in the nearby Atlantic, but unfortunately this is one of the open issues, as outlined in Section I.17. However, the negative halosteric effect is generally much smaller than the currently predicted value of the positive contribution due to ice melting, and a substantial sea-level increase in the Mediterranean is supported by the large majority of model simulations.

The long-term evolution of marine storminess has been simulated under the IPCC future greenhouse gas emission scenarios. Marine storminess includes the superposition of the effects of waves and storm surges, as both are produced by intense air–sea interaction during meteorological events. Moreover, they are strongly modulated by mean sea-level rise, as this can compensate or reinforce the effects due to changes in storm regimes. The projection of sea-level extremes requires running a barotropic sea-level model forced by atmospheric pressure and wind fields obtained under different scenarios; the uncertainty associated with the storm-surge model is assumed to be small as compared with that of the forcing fields. A similar situation holds for the wind-generated ocean waves. Concerning meteorological events, model projections suggest a small decrease (Lionello et al., 2002, 2007), which would cause a decrease in the mean and extreme SWH (with only a few exceptions) (Lionello et al., 2008). A particularly interesting case is the shallow northern Adriatic, with its flat coastline, where no major increase of storm surge and wind waves is currently projected

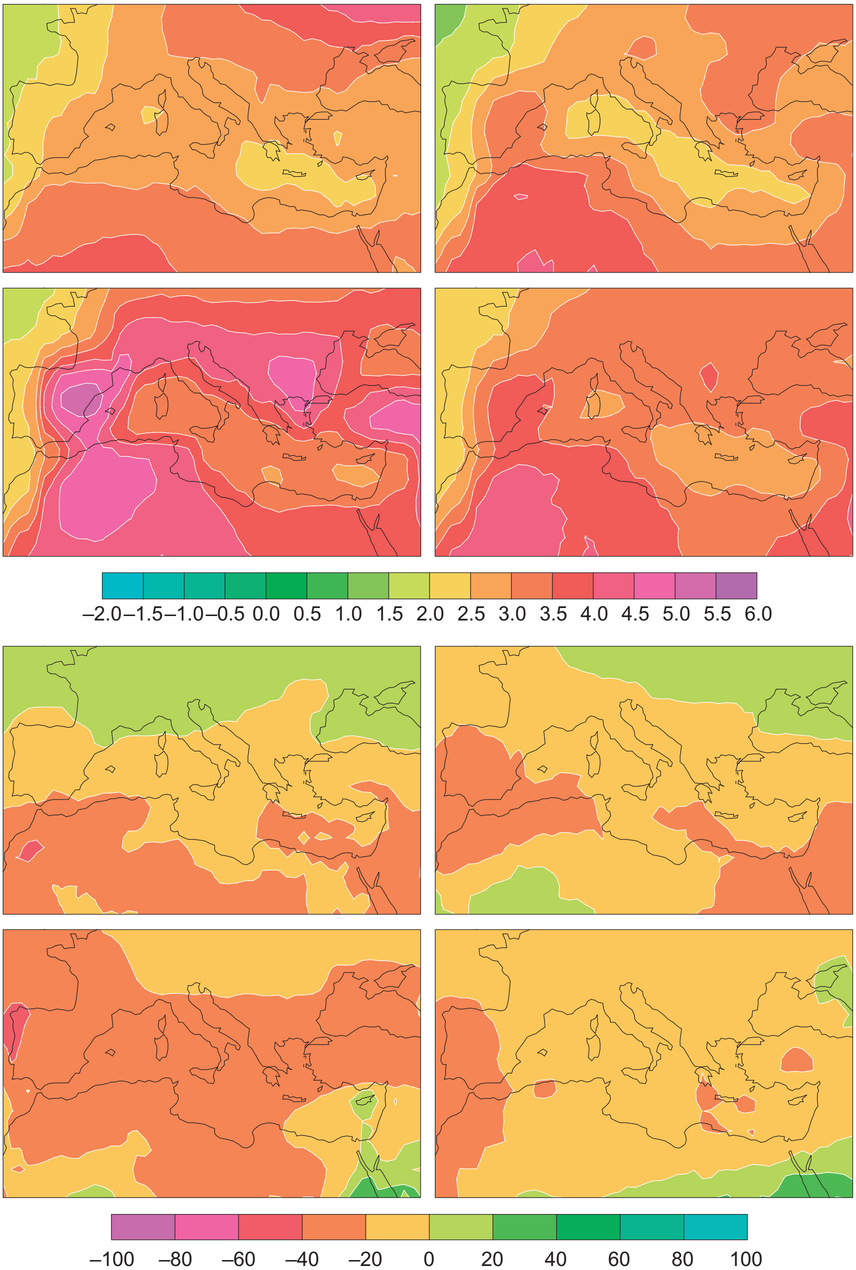

Figure I.20 Seasonal (DJF, MAM, JJA, SON) map of temperature (K, top panels) and precipitation signal (percent of the value in the reference period) climate change as resulting from an ensemble of GCMs. The maps show the differences between the 2071–2100 period of the A1B scenario and the reference period 1961–1990.
Source: Adapted from Giorgi and Lionello (2008).

(Lionello et al., 2010). However, Gaertner et al. (2007) have shown a large spread among the number of cyclones generated by different RCM projections, which would imply a large spread in the number of extreme marine storms.

From the Mediterranean-dedicated climate-change studies (see above), we conclude that the Mediterranean climate would become progressively warmer, drier, and likely, less windy in the twenty-first century. This would have an impact on the salinity (saltier) and temperature (warmer) of the surface waters, with an uncertain overall impact on density (because of the contrasting effect of the increase of salinity and temperature), on deep-water formation inside the basin, and on the exchanges between Mediterranean Sea and Atlantic Ocean through the Strait of Gibraltar. The changes of the near-Atlantic surface waters and of the river runoff would probably also modulate the impact of the climate change on the Mediterranean Sea. However, up to now, very few studies were really dedicated to the study of the possible evolution of the Mediterranean Sea in the twenty-first century. Marcos and Tsimplis (2008) demonstrated that the Mediterranean Sea was badly represented in the Coupled Model Intercomparison Project, phase 3 (CMIP3) GCM (see also Chapter 7). Too low resolution in the atmosphere forcing, in the Mediterranean Sea bathymetry and straits, and in the river catchment basin leads to suspicious results concerning the Mediterranean Sea evolution that is derived from GCM simulations.

A pioneer work using a high-resolution Mediterranean model was done by Thorpe and Bigg (2000) simulating a transient $2 \times CO_2$ scenario with a 1/4° resolution ocean model forced by very-low-resolution air–sea fluxes. Later, Somot et al. (2006) performed a similar study using a higher-resolution ocean model (1/8°) forced by fluxes coming from a dynamical downscaling (50 km) of an A2 IPCC run. For the first time, Somot et al. (2008) also used an Atmosphere-Ocean Regional Climate Model (AORCM) with online coupling between a regional atmospheric model and a regional ocean model perform a transient A2 scenario simulation. These new simulations allow better documentation of the impact of climate change on Mediterranean Sea circulation, including its thermohaline component. Further details are given in Chapter 8.

The level of confidence we can attribute to projections is also dependent on the ability of the climate models to reproduce observed variability and trends. Among the various strategies that can be used to check this ability, the detection of a simulated climate change in recent observations is of particular interest. It is indeed a way to evaluate the consistency between climate simulations and observation at timescales that are relevant to anthropogenic climate change (i.e., for a couple of decades). It is also, of course, of scientific and societal interest, since we would like to know whether some anthropogenic signal might be detected in recent climate observations.

According to the IPCC AR4, difficulties remain in attributing temperature changes to different causes on smaller than continental scales (Hegerl et al., 2007). This is in particular linked to the difficulties of models to reproduce regional-scale features. In the case of the Mediterranean area, this is also due to a lack of long data series of sufficient quality covering a significant part of the domain. However, a few studies analyzing temperature changes over southern Europe and over the Mediterranean domain have been performed allowing us to draw some clear conclusions (see Chapter 8). The main finding is that an anthropogenic signal can be detected in annual, winter, and summer temperature changes. Unfortunately, this conclusion cannot be drawn for precipitation because observation and modeling are even more challenging for this variable than they are for temperature. Thus, we cannot conclude at present whether what is observed for precipitation is due to internal climate variability or to some external forcing, in particular of human origin, such as changes of atmospheric composition.

I.17 Major Open Issues

It is the aim of this book to attempt an assessment of what is and what is not known about the Mediterranean climate. Much is known both about its past and its future evolution, about its present state, and about the processes responsible for its variability. The previous sections of this introduction and material in the following chapters allow a good assessment of the large amount of knowledge that is available. However, much is not known, and the rest of this section lists major open issues.

I.17.1 Paleoclimate Reconstructions

The resolution achieved for the different timescales is mainly a function of the quality and resolution of the climatic archive. In general terms, resolution and confidence in the data increase toward the present day, but despite this, uncertainty becomes more problematic for high-resolution and/or more recent reconstructions; work to quantify this uncertainty is still in its infancy. However, despite the associated uncertainties, paleoclimatic records are fundamental to examine the causes of past climate variability and to validate model simulations of past climate, which in turn can help us to improve the capacity to simulate future climate.

Examples of important questions to be asked include: What is different in the last 10 ky with respect to previous interglacials? Why were previous interglacials wetter? Integrating proxy data and their uncertainties in regional paleoclimate modeling is in fact the aim of several international modeling projects, which use multiple proxy types and multiple locations in space and time. As stated by Hughes et al. (2010), paleoclimatologists are faced with the need to find ways to incorporate the emerging techniques and concepts to improve reconstructions of past climate and to make more comprehensive estimates of the uncertainties associated with them.

I.17.2 Historical Climatology

In the Mediterranean, water availability is of major importance to societies and ecosystems strongly influence and stress human and natural systems, but currently we are still far from quantifying variations in the hydrological cycle–temperature changes at different time and space scales and from understanding the underlying mechanisms responsible for the observed changes over the past 2000 years. Are present conditions unprecedented in historical time? Are LIA and MCA clearly identified and properly characterized in the different parts of the Mediterranean region?

In order to answer these and similar questions, apart from a more improved proxy network, which can resolve the full range of climate variations at intraannual and interdecadal timescales, sophisticated statistical methods are necessary for assimilating proxy and instrumental data in order to estimate climate variables through time on a regular spatial grid covering the entire Mediterranean region.

I.17.3 Present Trends in Precipitation

Are trends in precipitation robust? Are they a first indication of climate change? Or is it just multidecadal variability? Are precipitation extremes changing? Is this a relevant issue, or does assessing their values and variability remain the main issue? These questions involve the recovery of many instrumental data time series, which exist in many locations in the Mediterranean region, and their comparison with the climate-change patterns produced by climate models. This is an ongoing effort whose results have not been conclusive so far.

I.17.4 Water Budget

Despite a fairly accurate conceptual scheme of the water cycle at the Mediterranean basin scale, the individual terms of the budget are difficult to determine accurately and a closure of the budget has not yet been obtained by summing the present estimates. These considerations lead to the conclusion that further research, concerning all physical compartments, is needed in order to allow a characterization of the mean components of the Mediterranean Sea water budget as well as of its seasonal, interannual, and decadal variability. The estimate of the river runoff is a critical part of this issue.

I.17.5 Sea Level and Circulation

The reconstruction of sea-level fields is based on coastal stations that are mostly located in the northwestern part of the basin. Although the basin mean sea-level trends are considered to be reasonably accurate, the trends estimated for the different sea-level components are more uncertain, particularly for steric sea level. The reason is the sparse spatiotemporal distribution of hydrographic data. Regional models should help to diagnose steric sea level, but at present, they suffer from drifts linked with the uncertainties in the freshwater and heat fluxes used to force the models. Other issues under discussion are land movements and the link between coastal and open sea level. Regarding Mediterranean circulation, the occurrence of different states of the thermohaline circulation is not yet documented and the probability of multiple equilibria of thermohaline cells has not been assessed.

I.17.6 The Role of Aerosols

Multiple processes affecting the regional Mediterranean climate and caused by abundant desert dust and pollution aerosols have been identified: radiative heating in the aerosol column, evaporation decrease at the sea surface, decrease in cloud-droplet radius, and enhancement of precipitation rates in convective continental clouds by mixing mineral dust with soluble salts forming giant CCN. First model estimates of such forcings indicate likely significant impacts on the regional climate. However, these physical processes and the full aerosol cycle remain to be implemented in ocean–atmosphere coupled regional climate models in order to assess their climate consequences and feedbacks. Furthermore, models of the tropospheric aerosol cycle are still facing a number of challenges to simulate the high variability in natural and anthropogenic particle concentrations in the Mediterranean region and in their optical and hygroscopic properties. Underconstrained emissions (e.g., from anthropogenic sources in north Africa, Mediterranean vegetation, forest fires, and arid areas) and underconstrained chemical and microphysical schemes (e.g., for computing secondary organic particle formation, light-absorption properties of aerosol particles, cloud properties, and precipitation) are especially critical. Those issues need to be resolved if we want to decipher the natural and anthropogenic aerosol forcing on the present Mediterranean climate and improve the reliability of climate projections.

I.17.7 Climate Projections

Dynamical downscaling techniques for all the components of the Mediterranean climate system seem to be required in order to assess the response of the Mediterranean Sea to climate change. Despite ongoing national efforts, we are still missing a large and coordinated ensemble of climate-change scenarios for the Mediterranean Sea to tackle the issue of the uncertainties in such simulations and improve confidence in projection of seasonal precipitation and its extremes such as floods and droughts. Projections of future sea level suffer from particularly large uncertainties. The global factor of the water-mass addition due to massive ice-cap melting is a major unknown, but it is not the only one. As stated above, understanding the role of the Strait of Gibraltar is crucial to link sea level in the Mediterranean with that in the nearby Atlantic, particularly in the present scenario, in which Mediterranean sea level seems to drift away from Atlantic sea level. Changes in the role of the Strait of Gibraltar in the future and of the exchanges through it are also a major issue.

I.17.8 Information for Climate-Change Impacts

Unfortunately, climatologists are not able to compare the future with the past and present climates with the level of accuracy and certainty that is required for analyzing impacts on ecosystems, societies, and regional economies. The timescale of regional climate change is crucial information in this respect. Studies of impacts and adaptation strategies on forestry, coastal environments, fisheries, agriculture, tourism, energy consumption, and water management should be very cautious, as they often rely on details of the future scenarios that are still quantitatively uncertain.

I.17.9 Outlook

An important basic motivation for climate studies is that regional climatic and environmental fluctuations affect societies and ecosystems, and their understanding forms the basis for efficient adaptation and protection strategies. Uncertainties about Mediterranean climate affect both its past and its future. Despite significant scientific progress over the past two decades, there is still insufficient knowledge about the detailed sequence of changes related to regional climate forcings, internal variability, system feedbacks, and the responses of surface climate, land cover, and biosphere and hydrosphere during the past centuries. Uncertainties about climate change in the twenty-first century are also large and are due to a lack of understanding of the complexity of the climate system and our incapability of reaching an accurate high-resolution description on a regional scale. Uncertainties about analysis of socioeconomic impacts and adaptation strategies are further amplified by the large uncertainty about societal components of vulnerability: How fast will Middle East and north African countries become less dependent on the agricultural sector? How fast will they take up adaptation options? How quickly will they catch up in terms of science and technology, and will they have a political leadership seeking efficiently rational solutions? To address these questions is certainly not the task of climatologists, but they have to be aware, aside from the fascination of the intellectual questions that they try to answer, of the relevance of their results for human societies and management of the environment.

This book is a major result of the efforts of many scientists who contributed to the MedCLIVAR project. The project has built a network of scientists with complementary expertise, making possible a comprehensive approach to the description of the Mediterranean climate. This book, and specifically this introduction, reflects the need to develop a view of the regional climate that accounts for its different components and for the different timescales involved in its evolution. The concept expressed by this project is that it is important to share information among complementary topics and to understand their different methods and problems. At the same time, it is important to discuss in detail all specific problems within each topic and provide a synthesis of the present state of the art. Altogether, these considerations point to the general theme of integration of different topics into a regional Earth system.

Acknowledgments

The authors thank P. Malanotte and A. Busalacchi for their constructive review and the improvement of this chapter. Furthermore, the authors thank the ICARE data and processing center for the processing of MSG/SEVIRI data (http://www.icare.univ-lille1.fr/msg/browse). E. Xoplaki and A. Toreti acknowledge support by the EU FP6 IP CIRCE and EU FP7 IP ACQWA.

References

Abrantes, F., Mix, A., 1999. Reconstruction Ocean History—A Window into the Future. Plenum, New York, p. 437.

Ackerman, A.S., Toon, O.B., Stevens, D.E., Heymsfield, A.J., Ramanathan, V., Welton, E.J., 2000. Reduction of tropical cloudiness by soot. Science 288, 1042–1047.

Albrecht, B.A., 1989. Aerosols, cloud microphysics, and fractional cloudiness. Science 245, 1227–1230.

Alexander, L.V., Zhang, X., Peterson, T.C., Caesar, J., Gleason, B., Klein Tank, A.M.G., et al., 2006. Global observed changes in daily climate extremes of temperature and precipitation. J. Geophys. Res. 111, D05109. doi: 10.1029/2005JD006290.

Alpert, P., Ziv, B., 1989. The Sharav cyclone, observations and some theoretical considerations. J. Geophys. Res. 94, 18495–18514.

Alpert, P., Halfon, N., Levin, Z., 2008. Does air pollution really suppress precipitation in Israel? J. Appl. Meteorol. Climatol. 47 (4), 933–943.

Alpert, P., Baldi, M., Ilani, R., Krichak, S., Price, C., Rodó, X., et al., 2006a. Chapter 2. Relations between climate variability in the Mediterranean region and the tropics: ENSO, south Asian and African monsoons, hurricanes and Saharan dust. Dev. Earth Environ. Sci. 4 (C), 149–177.

Alpert, P., Ilani, R., da-Silva, A., Rudack, A., Mandel, M., 2006b. Seasonal prediction for Israel winter precipitation based on northern Hemispheric EOF, MERCHAVIM special issue in honour of Prof. Arie Bitan, 397–412.

Amitai, Y., Lehahn, Y., Lazar, A., Heifetz, E., 2010. Surface circulation of the eastern Mediterranean Levantine basin: insights from analyzing 14 years of satellite altimetry data. J. Geophys. Res. 115, C10058. doi: 10.1029/2010JC006147.

Antoine, D., Nobileau, D., 2006. Recent increase of Saharan dust transport over the Mediterranean Sea, as revealed from ocean color satellite (SeaWiFS) observations. J. Geophys. Res. 111, D12214. doi: 10.1029/2005JD006795 , p. 19.

Aviad, Y., Kutiel, H., Lavee, H., 2007. Variation of dry days since last rain (DDSLR) as a measure of dryness along a climatic transect. J. Arid Environ. 73, 658–665.

Barnaba, F., Gobbi, G.P., 2004. Aerosol seasonal variability over the Mediterranean region and relative impact of maritime, continental and Saharan dust particles over the basin from MODIS data in the year 2001. Atmos. Chem. Phys. 4, 2367–2391.

Bartholy, J., Pongracz, R., Pattantyus-Abraham, M., 2009. Analyzing the genesis, intensity, and tracks of western Mediterranean cyclones. Theor. Appl. Climatol. 96, 133–144.

Behrenfeld, M.J., Falkowski, P.G., 1997. Photosynthetic rates derived from satellite-based chlorophyll concentration. Limnol. Oceanogr. 42, 1–20.

Bergamasco, A., Gačić, M., 1996. Baroclinic response of the Adriatic Sea to an episode of Bora wind. J. Phys. Oceanogr. 26, 1354–1369.

Bergametti, G., Gomes, L., Remoudaki, E., Desbois, M., Martin, D., Buat-Mènard, P., 1989. Present transport and deposition patterns of African dust to the North-Western Mediterranean. In: Leinen, M. Sarthein, M. (Eds.), Paleoclimatology and Paleometeorology: Modern and Past Patterns of Global Atmospheric Transport, Kluwer Academic Publisher, 5 Dordrecht, pp. 227–252.

Bergamo, A., Tafuro, A.M., Kinne, S., De Tomasi, F., Perrone, M.R., 2008. Monthly-averaged anthropogenic aerosol direct radiative forcing over the Mediterranean based on AERONET aerosol properties. Atmos. Chem. Phys. 8, 6995–7014.

Béthoux, J.P., 1981. Le phosphore et l'azote en Méditerranée, bilans et fertilité potentielle. Mar. Chem. 10, 141–158.

Borzelli, G.L.E., Gačić, M., Cardin, V., Civitarese, G., 2009. Eastern Mediterranean Transient and reversal of the Ionian Sea circulation. Geophys. Res. Lett. 36, L15108. doi: 10.1029/2009GL039261.

Bradley, R.S., Hughes, M.K., Diaz, H.F., 2003. Climate in medieval time. Science 302, 404–405.

Bréon, F.-M., Tanré, D., Generoso, S., 2002. Aerosol effect on cloud droplet size monitored from satellite. Science 295, 834–838.

Bréon, F.-M., Vermeulen, A., Descloitres, J., 2011. An evaluation of satellite aerosol products against sunphotometer measurements. Remote Sens. Environ. 115, 3102–3111. ISSN 0034-4257, 10.1016/j.rse.2011.06.017.

Bryden, H.L., Stommel, H.M., 1984. Limiting processes that determine basic features of the circulation in the Mediterranean Sea. Oceanol. Acta 7, 289–296.

Buzzi, A., Tibaldi, S., 1978. Cyclogenesis on the lee of Alps: a case study. Q-Q. J. R. Meteorol. Soc. 104, 171–287.

Buzzi, A., Richard, E., Romero, R., 2005. Summary report on MEDEX studies and scientific results on Mediterranean cyclones causing high impact weather. MEDEX Project. <http://medex.aemet.uib.es/index.html>.

Caddy, J.F., 1993. Contrast between recent fishery trends and evidence from nutrient enrichment in two large marine ecosystems: the Mediterranean and the Black Seas. In: Sherman, K. (Ed.), Large Marine Ecosystems: Stress, Mitigation, and Sustainability. AAAS, Washington, DC087168506X, pp. 137–147.

Calafat, F.M., Gomis, D., 2009. Reconstruction of Mediterranean Sea level fields for the period 1945–2000. Global Planet. Change 66 (3–4), 225–234.

Carlson, T.N., Benjamin, S.G., 1980. Radiative heating rates for Saharan dust. J. Atmos. Sci. 37, 193–213.

Carrion, J.S., Fernandez, S., Jimenez-Moreno, G., Fauquette, S., Gil-Romera, G., Gonzalez-Samperiz, P., et al., 2010. The historical origins of aridity and vegetation degradation in southeastern Spain. J. Arid Environ. 74, 731–736.

Caussinus, H., Mestre, O., 2004. Detection and correction of artificial shifts in climate series. Appl. Stat. J. Roy. St. C 53, 405–425.

Cavaleri, L., Bertotti, L., 2004. Accuracy of modelled wind and waves fields in enclosed seas. Tellus 56 (2), 167.

Charlson, R.J., Schwartz, S.E., Hales, J.M., Cess, R.D., Coakley J.A., Jr., Hansen, J.E., et al., 1992. Climate forcing by anthropogenic aerosols. Science 255, 423–430.

Christensen, J.H., Hewitson, B., Busuioc, A., Chen, A., Gao, X., Held, I., et al., 2007. Regional climate projections. In: Solomon, S., Qin, D., Manning, M., Chen, Z., Marquis, M., Averyt, K.B. (Eds.), Climate Change 2007: The Physical Science Basis. Contribution of Working Group I to the Fourth Assessment Report of the Intergovernmental Panel on Climate Change. Cambridge University Press, Cambridge, UK and New York, NY.

Chronis, T., Papadopoulos, V., Nikolopoulos, E. I., 2010. QuickSCAT observations of extreme wind events over the Mediterranean and Black Seas during 2000–2008. Int. J. Climatol. doi: 10.1002/joc.2213.

Chung, C.E., Ramanathan, V., Kim, D., Podgorny, I.A., 2005. Global anthropogenic aerosol direct forcing derived from satellite and ground-based observations. J. Geophys. Res. 110, D24207. doi: 10.1029/2005JD006356, p. 17.

Colombaroli, D., Marchetto, A., Tinner, W., 2007. Long-term interactions between Mediterranean climate, vegetation and fire regime at Lago di Massaciuccoli (Tuscany, Italy). J. Ecol. 95, 755–770.

DeMott, P.J., Sassen, K., Poellot, M.R., Baumgardner, D., Rogers, D.C., Brooks, S.D., et al., 2003. African dust aerosols as atmospheric ice nuclei. Geophys. Res. Lett. 30, 1732. doi: 10.1029/2003GL017410.

Dessens, J., Berthet, C., Sanchez, J.L., 2007. A point hailfall classification based on hailpad measurements: the ANELFA scale. Atmos. Res. 83, 132–139.

Dorman, C.E., Beardsley, R.C., Limeburner, R., 1995. Winds in the Strait of Gibraltar. Q. J. R. Meteor. Soc. 121, 1903–1921.

Dubief, J., 1959. Le climat du Sahara. Tome I: Les températures. Mém. Inst. Rech. Sah. (Alger) I (HS), 1–308.

Dugdale, R.C., Wilkerson, F.P., 1988. Nutrient sources and primary production in the eastern Mediterranean. Oceanol. Acta 9, 179–184. (special issue).

Dünkeloh, A., Jacobeit, J., 2003. Circulation dynamics of Mediterranean precipitation variability 1948–98. Int. J. Climatol. 23, 1843–1866.

Efthymiadis, D., Goodess, C.M., Jones, P.D., 2011. Trends in Mediterranean gridded temperature extremes and large-scale circulation influences. Nat. Hazards Earth Syst. Sci. 11, 2199–2214. doi: 10.5194/nhess-11-2199-2011.

Esper, J., Frank, D.C., Büntgen, U., Verstege, A., Luterbacher, J., Xoplaki, E., 2007. Long-term drought severity variations in Morocco. J. Geophys. Res. 108, 8059. doi: 10.1029/2001JC000825, 17 pp.

Estrada, M., 1999. Primary production in the northwestern Mediterranean. Sci. Mar. 60, 55–64.

Fernandez, S., ENGREF, 2007. L'eau virtuelle dans les pays méditerranéens: un indicateur pour contribuer à l'analyse des questions de gestion et de répartition de l'eau en situationde pénurie. Rapport d'étude régionale du Plan Bleu. www.planbleu.org/publications/eau_virtuelle_FR.pdf.

Fischer, G., Wefer, G., 1999. Use of Proxies in Paleoceanography: Examples from the south Atlantic. Springer, Berlin.

Fiuza, A., 1983. Upwelling patterns off Portugal In: Suess, E. Thiede, J. (Eds.), Coastal Upwelling its Sediment Record, vol. 1. Plenum, New York, pp. 85–98.

Flocas, A.A., 1988. Frontal depressions over the Mediterranean Sea and Central Southern Europe. Mediterranee 4, 43–52.

Formenti, P., Boucher, O., Reiner, T., Sprung, D., Andreae, M.O., Wendisch, M., et al., 2002. STAAARTE-MED 1998 summer airborne measurements over the Aegean Sea 2. Aerosol scattering and absorption, and radiative calculations. J. Geophys. Res. 107, 4451. doi: 10.1029/2001JD001536, p. 14.

Gaertner, M.A., Jacob, D., Gil, V., Domínguez, M., Padorno, E., Sánchez, E., et al., 2007. Tropical cyclones over the Mediterranean Sea in climate change simulations. Geophys. Res. Lett. 34, L14711. doi: 10.1029/2007GL029977.

García-Lafuente, J., Sánchez-Roman, A., Del Río, G.D., Sannino, G., Sánchez-Garrido, J., 2007. Recent observations of seasonal variability of the Mediterranean outflow in the Strait of Gibraltar. J. Geophys. Res. 112, C10005. doi: 10.1029/2006JC003992.

Gimeno, L., Drumond, A., Nieto, R., Trigo, R.M., Stohl, A., 2010. On the origin of continental precipitation. Geophys. Res. Lett. 37, L13804. doi: 10.1029/2010GL043712.

Giorgi, F., 2006. Climate change hot-spots. Geophys. Res. Lett. 33, L08707.

Giorgi, F., Lionello, P., 2008. Climate change projections for the Mediterranean region. Global Planet. Change 63 (2–3), 90–104. doi: 10.1016/j.gloplacha.2007.09.005.

Gkikas, A., Hatzianastassiou, N., Mihalopoulos, N., 2009. Aerosol events in the broader Mediterranean basin based on 7-year (2000–2007) MODIS C005 data. Annal. Geophys. 27, 3509–3522.

Hadjimichael, M., Kuciauskas, A.P., Brody, L.R., Tag, P.M., Bankert, R.L., Peak, J.E., 2002. A meteorological fuzzy expert system incorporating subjective user input. Knowl. Inf. Syst. 4 (3), 350–369.

Haylock, M.R., Hofstra, N., Klein Tank, A.M.G., Klok, E.J., Jones, P.D., New, M., 2008. A European daily high-resolution gridded data set of surface temperature and precipitation for 1950–2006. J. Geophys. Res. 113, D20119. doi: 10.1029/2008JD010201.

Hegerl, G.C., Zwiers, F.W., Braconnot, P., Gillett, N.P., Luo, Y., Marengo Orsini, J.A., et al., 2007. Climate Change 2007: The Physical Science Basis. Contribution of Working Group I to the Fourth Assessment Report of the Intergovernmental Panel on Climate Change, chap. Understanding and Attributing Climate Change. Cambridge University Press, Cambridge, UK, pp. 663–745.

Herbaut, C., Mortier, L., Crepon, M., 1996. A sensitivity study of the general circulation of the western Mediterranean. Part I. The response to density forcing through the straits. J. Phys. Oceanogr. 26 (1), 65–84.

Hillaire-Marcel, C., De Vernal, A., 2007. Proxies in Late Cenozoic Paleoceanography. Developments in Marine Geology. Elsevier, Amsterdam.

Holben, B.N., Eck, T.F., Sluster, I., Tanré, D., Buis, J.P., Setzer, A., et al., 1998. AERONET-A federated instrument network and data archive for aerosol characterization. Remote Sens. Environ. 66, 1–16.

Homar, V., Jansa, A., Campins, J., Genoves, A., Ramis, C., 2007. Towards a systematic climatology of sensitivities of Mediterranean high impact weather: a contribution based on intense cyclones. Nat. Hazards Earth Syst. Sci. 7, 445–454.

Hughes, M.K., Guiot, J., Ammann, C.M., 2010. Emerging techniques and concepts offer ways to improve the use of process knowledge in reconstructions of past climate, and to make more comprehensive estimates of the uncertainties associated with them. PAGES News 18, 87–89.

IAASTD, 2008. International Assessment of Agricultural Knowledge, Science and Technology for Development, Central and West Asia and North Africa, Summary for Decision Makers. <http://www.agassessment.org/docs/IAASTD_EXEC_SUMMARY_JAN_2008.pdf>

Isono, K., Komabayasi, M., Ono, A., 1959. The nature and the origin of ice nuclei in the atmosphere. J. Meteorol. Soc. Jpn. 37, 211–233.

Johnson, B.T., Shine, K.P., Forster, P., 2004. The semi-direct aerosol effect: impact of absorbing aerosols on marine stratocumulus. Q. J. R. Meteorol. Soc. 130, 1407–1422.

Jouzel, J., Masson-Delmotte, V., Cattani, O., Dreyfus, G., Falourd, S., Hoffmann, G., et al., 2007. Orbital and millennial Antarctic climate variability over the past 800,000 years. Science 317, 793–796.

Knippertz, P., Ulbrich, U., Marques, F., Corte-Real, J., 2003. Decadal changes in the link El Niño, NAO and European/north African rainfall. Int. J. Climatol. 23, 1293–1311.

Köppen, W., 1900. Versuch einer klassifikation der klimate, vorzugsweise nach ihren beziehungen zur pflanzenwelt. Geogr. Z. 6, 593–611. 657–679.

Kourafalou, V.H., Barbopoulos, K., 2003. High resolution simulations on the north Aegean Sea seasonal circulation. Annal. Geophys. 21, 251–265.

Kuglitsch, F.G., Toreti, A., Xoplaki, E., Della-Marta, P.M., Zerefos, C.S., Türkeş, M., et al., 2010. Heat wave changes in the eastern Mediterranean since 1960. Geophys. Res. Lett. 37, L04802. doi: 10.1029/2009GL041841.

Lacombe, H., Tchernia, P., 1972. Charactéres hydrologiques et circulation des eaux en Méditerranée. In: Stanley, D.J. (Ed.), The Mediterranean Sea. Dowden, Hutchinson, and Ross, Stroudsburg, PA, pp. 26–36.

Lascaratos, A., 1992. Hydrology of the Aegean Sea. In: Charnock, H. (Ed.), Winds and Currents of the Mediterranean Basin, Reports in Meteorology and Oceanography, vol. 40(1), Harvard University, Cambridge, pp. 313–334.

Lelieveld, J., Berresheim, H., Borrmann, S., Crutzen, P.J., Dentener, F.J., Fischer, H., et al., 2002. Global air pollution crossroads over the Mediterranean. Science 298, 794–799.

Léon, J.-F., Chazette, P., Pelon, J., Dulac, F., Randriamiarisoa, H., 2002. Aerosol direct radiative impact over the INDOEX area based on passive and active remote sensing. J. Geophys. Res. 107. doi: 10.1029/2000JD000116, p. 10.

Le Treut, H., Le Forichon, M., Boucher, O., Li, Z.-X., 1998. Sulfate aerosol indirect effect and CO_2 greenhouse forcing: equilibrium response of the LMD GCM and associated cloud feedbacks. J. Climate 11, 1673–1684.

Levin, Z., Ganor, E., Gladstein, V., 1996. The effects of desert particles coated with sulphate on rain formation in the eastern Mediterranean. J. Appl. Meteor. 35, 1511–1523.

Levin, Z., Teller, A., Ganor, E., Yin, Y., 2005. On the interactions of mineral dust, sea-salt particles, and clouds: a measurement and modeling study from the Mediterranean Israeli Dust Experiment campaign. J. Geophys. Res. 110, D20202. doi: 10.1029/2005JD005810.

Levitus, S., Antonov, J.I., Boyer, T.P., Locarnini, R.A., García, H.E., Mishonov, A.V., 2009. Global ocean heat content 1955–2008 in light of recently revealed instrumentation problems. Geophys. Res. Lett. 36, L07608. doi: 10.1029/2008GL037155.

Lionello, P., 2005. Extreme surges in the Gulf of Venice. Present and future climate. In: Fletcher, C., Spencer, T. (Eds.), Venice and its Lagoon, State of Knowledge Cambridge University Press, Cambridge, UK, pp. 59–65.

Lionello, P., Sanna, A., 2005. Mediterranean wave climate variability and its links with NAO and Indian monsoon. Clim. Dyn. 25, 611–623.

Lionello, P., Galati, M.B., 2008. Links of the significant wave height distribution in the Mediterranean Sea with the north hemisphere teleconnection patterns. Adv. Geosci. 17, 13–18.

Lionello, P., Dalan, F., Elvini, E., 2002. Cyclones in the Mediterranean region: the present and the doubled CO_2 climate scenarios. Clim. Res. 22, 147–159.

Lionello, P., Boldrin, U., Giorgi, F., 2007. Future changes in cyclone climatology over Europe as inferred from a regional climate simulation. Clim. Dyn. doi: 10.1007/s00382-007-0315-0.

Lionello, P., Galati, M.B., Elvini, E., 2010. Extreme storm surge and wind wave climate scenario simulations at the Venetian littoral. Phys. Chem. Earth. doi: 10.1016/j.pce.2010.04.001.

Lionello, P., Cogo, S., Galati, M.B., Sanna, A., 2008. The Mediterranean surface wave climate inferred from future scenario simulations. Global Planet. Change. doi: 10.1016/j.gloplacha.2008.03.004.

Lionello, P., Bhend, J., Buzzi, A., Della-Marta, P.M., Krichak, S., Jansà, A., et al., 2006b. Cyclones in the Mediterranean region: climatology and effects on the environment. Dev. Earth Environ. Sci. 4 (C)), 325–372.

Lionello, P., Malanotte-Rizzoli, P., Boscolo, R., Alpert, P., Artale, V., Li, L., et al., 2006a. The Mediterranean climate: an overview of the main characteristics and issues. Dev. Earth Environ. Sci. 4 (C), 1–26.

Losada, A.M., 1999. Analysis of the meteorological synoptic situations that affect the Straits of Gibraltar and their influence on the surface wind. Bol. Inst. Esp. Oceanogr. 15 (1–4), 81–90.

Ludwig, W., Dumont, E., Meybeck, M., Heussner, S., 2009. River discharges of water and nutrients to the Mediterranean and Black Sea: major drivers for ecosystem changes during past and future decades? Progr. Oceanogr. 80, 199–217.

Luterbacher, J., Xoplaki, E., Casty, C., Wanner, H., Pauling, A., Kuttel, M., et al., 2006. Mediterranean climate variability over the last centuries: a review. In: Lionello, P., Malanotte-Rizzoli, P., Boscolo, R. (Eds.), The Mediterranean Climate: An Overview of the Main Characteristics and Issues. Elsevier, Amsterdam, pp. 27–148.

Luterbacher, J., García-Herrera, R., Akcer-On, S., Allan, R., Alvarez-Castro, M.C., Benito, G., et al., 2012. A review of 2000 years of paleoclimatic evidence in the Mediterranean. The Climate of the Mediterranean Region, 87–183.

Maheras, P., 1980. Le probleme des Etesiens. Mediterranee 40, 57–66.

Malanotte-Rizzoli, P., Bergamasco, A., 1989. The wind and thermally-driven circulation of the eastern Mediterranean. Part I. Oceanol. Acta 12 (4), 335–351.

Mann, M.E., Zhang, Z., Rutherford, S., Bradley, R.S., Hughes, M.K., Shindell, D., et al., 2009. Global signatures and dynamical origins of the little ice age and medieval climate anomaly. Science 326, 1256–1260.

Marcos, M., Tsimplis, M., 2008. Comparison of results of AOGCMs in the Mediterranean Sea during the 21st century. J. Geophys. Res. 113, C12028. doi: 10.1029/2008JC004820.

Margalef, R., Castellví, J., 1967. Fitoplancton y producción primaria de la costa catalana, de julio de 1966 a julio de 1967. Inv. Pesq. 31, 491–502.

Mariotti, A., Zeng, N., Lau, K.M., 2002a. Euro-Mediterranean rainfall and ENSO—a seasonally varying relationship. Geophys. Res. Lett. 29, 1621.

Mariotti, A., Struglia, M.V., Zeng, N., Lau, K.-M., 2002b. The hydrological cycle in the Mediterranean region and implications for the water budget of the Mediterranean Sea. J. Clim. 15, 1674–1690. doi: 10.1175/1520-0442(2002)015.

Markowicz, K.M., Flatau, P.J., Ramana, M.V., Crutzen, P.J., Ramanathan, V., 2002. Absorbing Mediterranean aerosols lead to a large reduction in the solar radiation at the surface. Geophys. Res. Lett. 29, 1968. doi: 10.1029/2002GL015767, p. 4.

Mason, B.J., Maybank, J., 1958. Ice-nucleating properties of some natural mineral dusts. Q. J. R. Meteor. Soc. 84, 235–241.

McCall, J.M., 2008. Primary production and marine fisheries associated with the Nile outflow. Earth Environ. 3, 179–208.

McGranahan, G., Balk, D., Anderson, B., 2007. Climate change and the risk of settlement in the low elevation coastal zone. IHDP update 2007:12–14; World Bank, 1999. World Development Report. Washington, DC.

MEDAR Group, 2002. Mediterranean and Black Sea Database of Temperature, Salinity and Biochemical Parameters and Climatological Atlas [CD-ROM]. Institut Français de Recherche pour l'Exploitation de la Mer, Plouzane, France. <http://www.ifremer.fr/sismer/program/medar/>.

Meloni, D., Di Sarra, A., Pace, G., Monteleone, F., 2006. Aerosol optical properties at Lampedusa (Central Mediterranean). Determination of single scattering albedo at two wavelengths for different aerosol types. Atmos. Chem. Phys. 6, 715–727.

Meloni, D., Di Sarra, A., DeLuisi, J., Di Iorio, T., Fiocco, G., Junkermann, W., et al., 2003. Tropospheric aerosols in the Mediterranean: 2. Radiative effects through model simulations and measurements. J. Geophys. Res. 108, 4317. doi: 10.1029/2002JD002807, pp. 16.

Millot, C., 1999. Circulation in the western Mediterranean Sea. J. Mar. Syst. 20, 423–442.

Millot, C., Taupier-Letage, I., 2005b. Additional evidence of LIW entrainment across the Algerian Basin by mesoscale eddies and not by a permanent westward-flowing vein. Progr. Oceanogr. 66, 231–250.

Minas, H.J., 1968. À propos d'une remontée d'eaux "profondes" dans les parages du golfe de Marseille (Octobre 1964). Conséquences biologiques. Cah. Océanogr. 20, 647–674.

Moulin, C., Lambert, C.E., Dulac, F., Dayan, U., 1997. Control of atmospheric export of dust from north Africa by the north Atlantic oscillation. Nature 387, 691–694.

Moulin, C., Lambert, C.E., Dayan, U., Masson, V., Ramonet, M., Bousquet, P., et al., 1998. Satellite climatology of African dust transport in the Mediterranean atmosphere. J. Geophys. Res. 103, 13137–13144.

New, M., Hulme, M., Jones, P.D., 1999. Representing twentieth century space-time climate variability. Part 1: development of a 1961–90 mean monthly terrestrial climatology. J. Clim. 12, 829–856.

New, M.G., Hulme, M., Jones, P.D., 2000. Representing twentieth century space time climate fields. Part II: development of a 1901–1996 mean monthly terrestrial climatology. J. Clim. 13, 2217–2238.

Nicholls, R.J., Wong, P.P., Burkett, V.R., Codignotto, J., Hay, J., McLean, R., et al., 2007. Coastal systems and low-lying areas. In: Parry, M.L., Canziani, O.F., Palutikof, J.P., van der Linden, P.J., Hanson, C.E. (Eds.), Climate Change 2007: Impacts, Adaptation and Vulnerability. Contribution of Working Group II to the Fourth Assessment Report of the Intergovernmental Panel on Climate Change. Cambridge University Press, Cambridge, UK, pp. 315–356.

Oki, Taikan, Sud, Y.C., 1998. Design of total runoff integrating pathways (TRIP)—a global river channel network. Earth Interact. 2, 1–37.

Pace, G., Meloni, D., Di Sarra, A., 2005. Forest fire aerosol over the Mediterranean basin during summer 2003. J. Geophys. Res. 110, D21202. doi: 10.1029/2005JD005986, p.11.

Paklar, G.B., Isakov, V., Koracin, D., Kourafalou, V., Orlic, M., 2001. A case study of bora-driven flow and density changes on the Adriatic shelf (January 1987). Cont. Shelf Res. 21, 1751–1783.

Papadimas, C.D., Hatzianastassiou, N., Mihalopoulos, N., Querol, X., Vardavas, I., 2008. Spatial and temporal variability in aerosol properties over the Mediterranean basin based on 6-year (2000–2006) MODIS data. J. Geophys. Res. 113, D11205. doi: 10.1029/2007JD009189, p. 12.

Papadimas, C.D., Hatzianastassiou, N., Mihalopoulos, N., Kanakidou, M., Katsoulis, B.D., Vardavas, I., 2009. Assessment of the MODIS Collections C005 and C004 aerosol optical depth products over the Mediterranean basin. Atmos. Chem. Phys. 9, 2987–2999.

Paz, S., Kutiel, H., 2003. Rainfall regime uncertainty (RRU) in an eastern Mediterranean region. A methodological approach. Israel J. Earth Sci. 52, 47–63.

Pinardi, N., Navarra, A., 1993. Baroclinic wind adjustment processes in the Mediterranean Sea. Deep Sea Res. II 40 (6), 1299–1326.

Plan Bleu, 2005. A Sustainable Future for the Mediterranean: The Blue Plan's Environment and Development Outlook. In: Benoit, G., Comeau, A. (Eds.), p. 464, Earthscan. <http://www.planbleu.org/red/pdf/red_resume_uk.pdf>

Plan Bleu, 2009. State of the Environment and Development. UNEP/MAP-Plan Bleu, Athens, 2009. <www.planbleu.org/publications/SoED2009_EN.pdf>.

Poulos, S., Drakopoulos, P., Collins, M., 1997. Seasonal variability in sea surface oceanographic conditions in the Aegean Sea (eastern Mediterranean): an overview. J. Mar. Syst. 13, 225–244.

Pruppacher, H.R., Klett, J.D., 1997. Microphysics of Clouds and Precipitation, second ed. Kluwer, Dordrecht, The Netherlands, p. 977.

Ramanathan, V., Crutzen, P.J., Lelieveld, J., Mitra, A.P., Althausen, D., Anderson, J., et al., 2001. Indian ocean experiment: an integrated analysis of the climate forcing and effects of the great Indo-Asian haze. J. Geophys. Res. 106, 28371–28398.

Reale, O., Shukla, J., 2000. Modeling the effects of vegetation on Mediterranean climate during the Roman classical period: Part II: model simulation. Global Planet 25, 185–214.

Reiser, H., Kutiel, H., 2010a. Rainfall uncertainty in the Mediterranean: intra-seasonal rainfall distribution. Theor. Appl. Climatol. 100, 105-121. doi: 10.1007/s00704-009-0162-5.
Reiser, H., Kutiel, H., 2010b. The impacts of the Rain-Spells' parameters on the annual TOTAL in the Mediterranean basin. Geogr. Ann. A. doi: 10.1111/j.1468-0459.2011.00444.x.
Rinaldi, E., Buongiorno Nardelli, B., Zambianchi, E., Santoleri, R., Poulain, P.-M., 2010. Lagrangian and Eulerian observations of the surface circulation in the Tyrrhenian Sea. J. Geophys. Res. 115, C04024. doi: 10.1029/2009JC005535.
Rixen, M., Bekers, J.-M., Levitus, S., Antonov, J., Boyer, T., Maillard, C., et al., 2005. The western Mediterranean deep water: a proxy for climate change. Geophys. Res. Lett. 32, L12608. doi: 10.1029/2005GL022702.
Roger, J.-C., Mallet, M., Dubuisson, P., Cachier, H., Vermote, E., Dubovik, O., et al., 2006. A synergetic approach for estimating the local direct aerosol forcing: application to an urban zone during the Expérience sur Site pour Contraindre les Modèles de Pollution et de Transport d'Emission (ESCOMPTE) experiment. J. Geophys. Res. 111, D13208. doi: 10.1029/2005JD006361, p. 9.
Roberts, N., Moreno, A., Valero-Garcés, B.L., Corella, J.P., Jones, M., Allcock, S., et al., 2012. Palaeolimnological evidence for an east–west climate see-saw in the Mediterranean since AD 900. Global Planet. Change 84–85, 23–34. ISSN 0921-8181, 10.1016/j.gloplacha.2011.11.002.
Roether, W., Klein, B., Manca, B.B., Thecharis, A., Kioroglou, S., 2007. Transient eastern Mediterranean deep waters in response to the massive dense water output of the Aegean Sea in the 1990s. Prog. Oceanogr. 74, 540–571.
Romanou, A., Tselioudis, G., Zerefos, C.S., Clayson, C.-A., Curry, J.A, Andersson, A., 2010. Evaporation—precipitation variability over the Mediterranean and the Black Seas from satellite and reanalysis estimates. J. Clim. doi: 10.1175/2010JCLI3525.1.
Rosenfeld, D., Rudich, Y., Lahav, R., 2001. Desert dust suppressing precipitation: a possible desertification feedback loop. Proc. Natl. Acad. Sci. USA 98, 5975–5980.
Roussenov, V., Stanev, E., Artale, V., Pinardi, N., 1995. A seasonal model of the Mediterranean Sea general circulation. J. Geophys. Res. 100, 13515–13538.
Ruddiman, W.F., 2007.. In: Ruddiman, W.F. (Ed.), Earth's Climate: Past and Future, second ed.. W. H. Freeman, New York.
San Feliu, J.M., Muñoz, F., 1971. Fluctuations d'une année à l'autre dans l'intensité de l'affleurement dans la Méditerranée occidentale. Inv. Pesq. 35, 155–159.
Sangati, M., Borga, M., 2009. Influence of rainfall spatial resolution on flash flood modelling. Nat. Hazard Earth Syst. Sci. 9, 575–584.
Santese, M., De Tomasi, F., Perrone, M.R., 2007. Moderate resolution imaging spectroradiometer (MODIS) and aerosol robotic network (AERONET) retrievals during dust outbreaks over the Mediterranean. J. Geophys. Res. 112, D18201. doi: 10.1029/2007JD008482, p. 14.
Somot, S., Sevault, F., Déqué, M., 2006. Transient climate change scenario simulation of the Mediterranean Sea for the 21st century using a high-resolution ocean circulation model. Clim. Dyn. 27 (7–8), 851–879. doi: 10.1007/s00382-006-0167-z.
Somot, S., Sevault, F., Déqué, M., Crépon, M., 2008. 21st century climate change scenario for the Mediterranean using a coupled atmosphere − ocean regional climate model. Global Planet. Change 63 (2–3), 112–126. doi: 10.1016/j.gloplacha.2007.10.003.
Struglia, M.V., Mariotti, A., Filograsso, A., 2004. River discharge into the Mediterranean Sea: climatology and aspects of the observed variability. J. Clim. 17, 4740–4751.
Textor, C., Schulz, M., Guibert, S., Kinne, S., Balkanski, Y., Bauer, YS., et al., 2006. Analysis and quantification of the diversities of aerosol life cycles within AeroCom. Atmos. Chem. Phys. 6, 1777–1813.

Thieuleux, F., Moulin, C., Bréon, F.M., Maignan, F., Poitou, J., Tanré, D., 2005. Remote sensing of aerosols over the oceans using MSG/SEVIRI imagery. Annal. Geophys. 23, 1–8.

Thorpe, R., Bigg, G., 2000. Modelling the sensitivity of the Mediterranean outflow to anthropogenically forced climate change. Clim. Dyn. 16, 355–368.

Tomczak, M., 1999. Some historical, theoretical and applied aspects of quantitative water mass analysis. J. Mar. Res. 57, 275–303.

Toreti, A., Xoplaki, E., Maraun, D., Kuglitsch, F.G., Wanner, H., Luterbacher, J., 2010. Characterisation of extreme winter precipitation in the Mediterranean and associated anomalous atmospheric circulation patterns. Nat. Hazard Earth Syst. 10, 1037–1050.

Toreti, A., Kuglitsch, F.G., Xoplaki, E., Luterbacher, J., 2012. A novel approach for the detection of inhomogeneities affecting climate time series. J. Appl. Meteorol. Climatol. 51 (2), 317–326.

Tragou, E., Lascaratos, A., 2003. Role of aerosols on the Mediterranean solar radiation. J. Geophys. Res. 108, 3025. doi: 10.1029/2001JC001258, p. 13.

Trigo, I.F., Davies, T.D., 2002. Meteorological conditions associated with sea surges in Venice: a 40 year climatology. Int. J. Climatol. 22, 787–803.

Trigo, I.F., Davies, T.D., Bigg, G.R., 2000a. Decline in Mediterranean rainfall caused by weakening of Mediterranean cyclones. Geophys. Res. Lett. 27, 2913–2916.

Trigo, I.F., Davies, T.D., Bigg, G.R., 2000b. Objective climatology of cyclones in the Mediterranean region. J. Clim. 12, 1685–1696.

Trigo, R., Xoplaki, E., Zorita, E., Luterbacher, J., Krichak, S.O., Alpert, P., et al., 2006. Chapter 3. Relations between variability in the Mediterranean region and mid-latitude variability. Dev. Earth Environ. Sci. 4 (C), 179–226.

Twomey, S., 1974. Pollution and the planetary albedo. Atmos. Environ. 8, 1251–1256.

Uppala, S.M., KÅllberg, P.W., Simmons, A.J., Andrae, U., Da Costa Bechtold, V., Fiorino, M., et al., 2005. The ERA-40 reanalysis. Q. J. R. Meteorol. Soc. 131, 2961–3012. doi: 10.1256/qj.04. 176.

Viúdez, A., Tintoré, J., Haney, R.L., 1996a. Circulation in the Alboran Sea as determined by quasi-synoptic hydrographic observations. Part I: three-dimensional structure of the two anticyclonic gyres. J. Phys. Oceanogr. 26, 684–705.

Viúdez, A., Haney, R.L., Tintoré, J., 1996b. Circulation in the Alboran Sea as determined by quasi-synoptic hydrographic observations. Part II: mesoscale ageostrophic motion diagnosed through density dynamical assimilation. J. Phys. Oceanogr. 26, 706–724.

Wiacek, A., Peter, T., Lohmann, U., 2010. The potential influence of Asian and African mineral dust on ice, mixed-phase and liquid water clouds. Atm. Chem. Phys. 10, 8649–8667. doi: 10.5194/acp-10-8649-2010.

Wurzler, S., Reisin, T.G., Levin, Z., 2000. Modification of mineral dust particles by cloud processing and subsequent effects on drop size distributions. J. Geophys. Res. 105, 4501–4512.

Xie, P., Arkin, P.A., 1996. Analyses of global monthly precipitation using gauge observations, satellite estimates, and numerical model predictions. J. Clim. 9, 840–858.

Xie, P., Arkin, P.A., 1997. Global precipitation: a 17-year monthly analysis based on gauge observations, satellite estimates, and numerical model outputs. B. Am. Meteorol. Soc. 78, 2539–2558.

Xoplaki, E., 2002. Climate variability over the Mediterranean, Ph.D. Thesis, University of Bern, Switzerland. <http://sinus.unibe.ch/klimet/docs/phd_xoplaki.pdf>.

Xoplaki, E., Fleitmann, D., Diaz, H., 2011. Editorial: medieval climate anomaly. PAGES News 19, 1ff.

Xoplaki, E., Gonzalez-Rouco, F. J., Luterbacher, J., Wanner, H., 2003. Mediterranean summer air temperature variability and its connection to the large-scale atmospheric circulation and SSTs. Clim. Dyn. 20, 723–739. doi: 10.1007/s00382-003–0304-x.

Xoplaki, E., Gonzalez-Rouco, F.J., Luterbacher, J., Wanner, H., 2004. Wet season Mediterranean precipitation variability: influence of large-scale dynamics. Clim. Dyn. 23, 63–78. doi: 10.1007/s00382-004–0422-0.

Xue, H., Feingold, G., 2006. Large-eddy simulations of trade wind cumuli: investigation of aerosol indirect effects. J. Atmos. Sci. 63, 1605–1622.

Yang, H., Wang, L., Zehnder, J.B., 2007. Water scarcity and food trade in the southern and eastern Mediterranean countries. Food Policy 32 (5–6), 585–605.

Yin, Y., Wurzler, S., Levin, Z., Reisin, T.G., 2002. Interactions of mineral dust particles and clouds: effects on precipitation and cloud optical properties. J. Geophys. Res. 107, 4724. doi: 10.1029/2001JD001544.

Zampieri, M., Lionello, P., 2011. Anthropic landuse cools down summer season in Europe. Clim. Res. 46, 255–268.

Zavatarelli, M., Mellor, G.L., 1995. A numerical study of the Mediterranean Sea circulation. J. Phys. Oceanogr. 46, 8–688.

Zimmermann, F., Weinbruch, S., Schütz, S., Hofmann, L., Ebert, H., Kandler, M., et al., 2008. Ice nucleation properties of the most abundant mineral dust phases. J. Geophys. Res. 113, D23204. doi: 10.1029/2008JD010655.

Link

http://www-pcmdi.llnl.gov
http://www.science.oregonstate.edu/ocean.productivity